Influence of Surface Groups on Poly(propylene imine) Dendrimers Anti-prion Activity

James M. McCarthy[1], Beatriz Rasines Moreno [2], Damien Filippini[2], Hartmut Komber[2], Marek Maly[3,4], Michaela Cernescu[5], Bernhard Brutschy[5], Dietmar Appelhans[2]*, Mark S. Rogers[1].*

[1] School of Biology and Environmental Science,

University College Dublin, Belfield, Dublin 4, Ireland.

[2] Leibniz Institute of Polymer Research Dresden, Hohe Str. 6, 01069 Dresden, Germany.

[3] J. E. Purkinje University, Ceske mladeze 8, 400 96 Usti nad Labem, Czech Republic.

[4] University of Applied Science of Southern Switzerland, Lab Appl Math & Phys LAMFI, CH-6928 Manno, Switzerland.

[5] Institute of Physical and Theoretical Chemistry, Johann-Wolfgang-Goethe University,

Max-von-Laue-Str. 7, D-60438 Frankfurt/Main, Germany.

* Corresponding authors: Dr. James M. McCarthy, School of Biology and Environmental Science, University College Dublin, Belfield, Dublin 4, Ireland. E-mail: jim.mccarthy@ucd.ie

Dr. Dietmar Appelhans, Leibniz Institute of Polymer Research Dresden, Hohe Strasse 6, D-01069 Dresden (Germany). E-mail: applhans@ipfdd.de

ABSTRACT

Prion diseases are characterized by the accumulation of PrP^{Sc}, an aberrantly folded isoform of the host protein PrP^{C}. Specific forms of synthetic molecules known as dendrimers are able to eliminate protease resistant PrP^{Sc} in both an intracellular and *in vitro* setting. The properties of a dendrimer which govern this ability are unknown. We addressed the issue by comparing the *in vitro* anti-prion ability of numerous modified poly(propylene-imine) dendrimers, which varied in size, structure, charge and surface group composition. Several of the modified dendrimers, including an anionic glycodendrimer, reduced the level of protease resistant PrP^{Sc} in a prion strain dependent manner. This led to the formulation of a new working model for dendrimer/prion interactions which proposes dendrimers eliminate PrP^{Sc} by destabilizing the protein and rendering it susceptible to proteolysis. This ability is not dependent on any particular charge of dendrimer but does require a high density of reactive surface groups.

KEYWORDS: Aggregate; Amyloid; Dendrimer; Neurodegenerative; Prion; Prion strain.

Introduction

Prion diseases are a group of fatal neurodegenerative diseases that include scrapie in sheep, bovine spongiform encephalopathy (BSE) in cattle, and Creutzfeldt-Jakob disease (CJD) in humans. Prion diseases can be infectious, genetic or sporadic in origin and are characterised by the accumulation of PrP^{Sc}, an aberrant structured form of the constitutively expressed cellular glycoprotein PrP^{C}. In comparison to PrP^{C}, PrP^{Sc} is insoluble and exists in protease sensitive and resistant forms.[1-5] The protein only hypothesis advocates that PrP^{Sc} is the major or sole constituent of the prion infectious agent[6, 7] and recent studies with recombinant PrP have supported this hypothesis.[8, 9] Prions exist in the form of different strains which differ in the brain regions they target and the incubation times and lesion profiles they induce in a particular host.[10-13] As prions are composed mainly or entirely of misfolded PrP protein, and replicate using the PrP substrate present in the host, differences in prion strains cannot be the result of genetic variability, which accounts for the existence of viral strains.[14] Instead, strain specific properties must be encoded by some feature of the pathogenic PrP other than its amino acid sequence, such as its conformation,[15, 16] its glycosylation pattern[17] or in unidentified PrP^{Sc} co-factors.[18] We recently demonstrated that a panel of synthetic polymers known as dendrimers can distinguish several prion strains against a common genetic background.[19] In this study those findings were expanded by investigating the molecular and chemical nature of the interactions that occur between different dendrimers and protease resistant PrP^{Sc} (PrP^{res}), with the ultimate aim of determining what features of a dendrimer govern it's *in vitro* anti-prion activity.

Dendrimers are synthetic polymers with a repeatedly branched, highly structured architecture. They generally consist of a core from which monomers branch out in a symmetrical, structured fashion, resulting in a spherical three dimensional morphology (Figure 1). Layers of monomers are attached stepwise during synthesis and the number of branch points defines the generation of dendrimer. The functional groups on the surface govern the ionic charge of the dendrimer. Numerous dendrimer

compounds have demonstrated anti-prion activity including the branched polyamines poly(propylene imine) (PPI), poly(amido amine) (PAMAM), poly(ethylene imine) (PEI),[20, 21] maltose based glycodendrimers (mPPI)[22, 23] and phosphorous dendrimers.[24] The ability of these dendrimers to eliminate PrP^{Sc} from infected cells is dose and time dependent and increases with the generation number of the dendrimer. In addition, mPPI, PPI, PAMAM and high MW PEI dendrimers are capable of eliminating protease resistant PrP^{Sc} from RML infected brain homogenate, making dendrimers the only known therapeutic to be effective against prions in both an intracellular and *in vitro* setting.[20, 21, 23]

The exact mechanism by which dendrimers achieve their *in vitro* effect is unknown but it has been shown that some dendrimers (PAMAM and pDADMAC) may bind to PrP^{Sc} under specified conditions of detergent and pH.[25] This binding is hypothesised to rely on multiple, mixed mode interactions, predominantly electrostatic and hydrophobic in nature. Aggregated abnormal forms of protein may have more binding sites available for interaction than non-aggregated versions of the protein, explaining the preference of dendrimers for misfolded and amyloid proteins.[25] The cationic dendrimers examined also selectively bound to tau aggregates.[25] Tau aggregates are encountered in the tauopathies, frontotemporal dementia, Alzheimer's disease and Parkinson's disease.[26-29] This suggests dendrimers may have potential in other protein misfolding diseases, a fact further enforced by dendrimers *in vitro* interaction with Aβ, a protein associated with Alzheimer's disease.[30-32]

Upon interaction, various dendrimers can alter the structure of proteins, particularly superficial, flexible regions of the polypeptide.[33] Polyamidoamine (PAMAM) dendrimers create a layer on the surface of albumin for example and change its conformation.[34] Dendrimers can also affect proteins' functions e.g. PAMAM affects acetylcholinesterase activity.[35] In the specific case of prions, different cationic dendrimers have been shown to disrupt prion fibrils, decrease their β-sheet content, and render protease resistant PrP^{Sc} (PrP^{res}) from prion infected brain homogenate susceptible to proteolysis.[20, 21, 36-38] The process is optimum at low pH and in the presence of urea suggesting that the denaturation of

PrP^{Sc} is involved in this process.[20, 21] The influence of dendrimers on protein aggregates may, at least in part, be attributed to a solvent effect. The dendrimer may act as a water structure perturbing solute (chaotrope), lowering the dielectric constant and the viscosity of water and disordering the regular water structure by reorganising the water molecules at the dendrimer surface which is in contact with the protein. As with other chaotropes, this would lead to hydrophobic interactions being disfavoured which is highly destabilizing for most protein tertiary structures.[39]

The anti-prion effect of most dendrimers is greatest when the dendrimer possesses a high cationic surface charge.[20, 24, 37] This led to speculation that the efficacy of a dendrimer in eliminating PrP^{Sc} was determined by its cationic charge density.[40] However, contrary to expectations, it was recently demonstrated that neutral maltose dendrimers exhibit anti-prion activity.[22, 23] This suggested that the polarity and structure of a dendrimer may also play an important role in dendrimer/PrP^{Sc} interactions. In this study these findings were extended, and the complex relationship governing dendrimer charge, structure and prion strain interactions explored. Our aim was to determine what features of a dendrimer define its *in vitro* anti-prion activity and to determine how these features differ according to prion strain. For this purpose, we took neutral maltose PPI dendrimers and introduced diverse peripheral groups with a wide variety of properties such as cationic, anionic and cationic/hydrophobic groups (Figure 1). These dendrimers were examined against a range of prion strains and their ability to reduce protease resistant PrP^{Sc} (PrP^{res}) assessed.

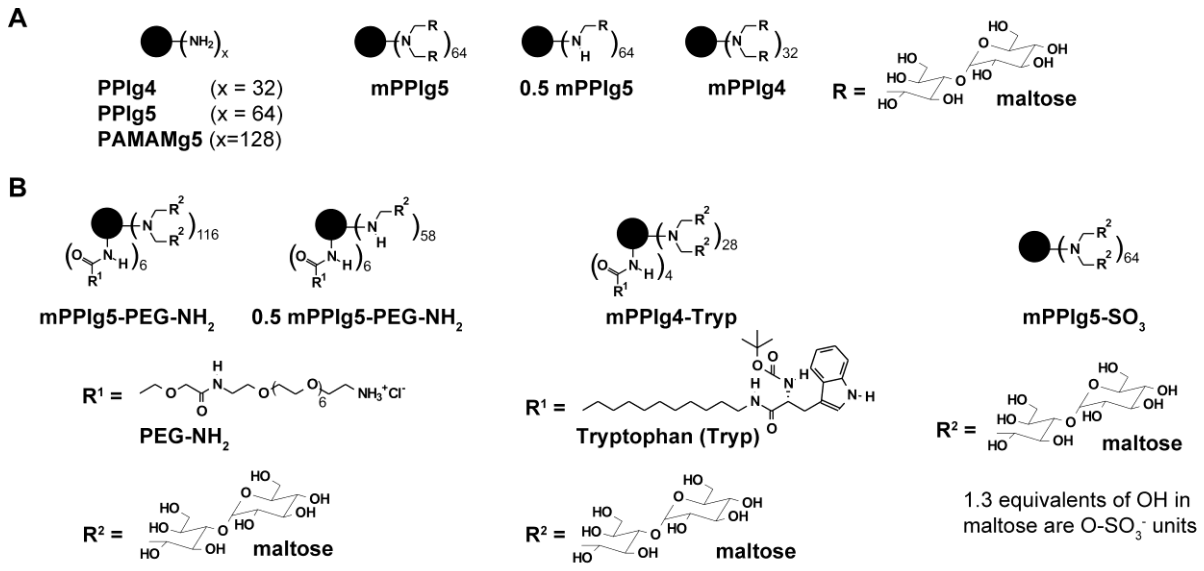

Glycodendrimer	Charge of base structure PPI dendrimer	Surface group	Charge of surface groups	Structure of glycodendrimers	Molecular weight *(g/mol)*
mPPIg5-PEG-NH_2	neutral	PEG-$NH_3^+Cl^-$	cationic	dense shell	40,720
0.5 mPPIg5-PEG-NH_2	cationic	PEG-$NH_3^+Cl^-$	cationic	open shell	25,600
mPPIg5-SO_3	neutral	sulphate	anionic	dense shell	59,000
mPPIg4-Tryp	neutral	tryptophan	cationic	dense shell	23,660

Figure 1. A) Core Dendrimers used in this study: Poly(propylene imine) generation four and five (PPIg4 and PPIg5), poly(amidoamine) generation five (PAMAMg5), dense maltose shell glycodendrimers generation four and five (mPPIg4 and mPPIg5) and open maltose shell glycodendrimer generation five (0.5 mPPIg5). **B) Novel dendrimers utilized in this study:** mPPIg5-PEG-NH_2 is a neutral mPPIg5 dendrimer modified through the addition of 6 $NH_3^+Cl^-$ surface groups on PEG spacers. 0.5 mPPIg5-PEG-NH_2 is a cationic 0.5 mPPIg5 dendrimer modified through the addition of 6 $NH_3^+Cl^-$ surface groups on PEG spacers. mPPIg4-Tryp is a neutral mPPIg4 dendrimer modified through the addition of 4 tryptophan groups on aliphatic spacers. mPPIg5-SO_3 is a neutral mPPIg5 dendrimer modified through the addition of 1-2 sulfate units per maltose unit in the outer shell of mPPIg5.

Experimental Section

Materials and Methods

Reagents: All reagents used were of analytical grade and unless otherwise stated, obtained from Sigma-Aldrich. Poly(propylene imine) dendrimers of 4th (PPIg4) and 5th (PPIg5) generation were obtained from SyMO-Chem (Eindhoven, Netherland). D(+)-maltose monohydrate and sodium borate (Fluka, Germany), borane*pyridine complex (BH_3*Py, 8 M solution in THF), sulfur trioxide*pyridine complex, 11-aminoundecanoic acid methyl ester hydrochloride, *N*α-(*tert*-butyloxycarbonyl)-L-tryptophan, benzotriazol-1-yloxy)tris(dimethylamino)phosphonium hexafluorophosphate (BOP) (Sigma, Germany), triethylamine (Acros, Germany) and α-tert-Butyloxycarbonylamino-ω-diglycolic acid-octa(ethylene glycol) (HO_2C-PEG-NHBoc) (Iris Biotech GmbH, Germany) were all used as purchased. Dendrimer stock compounds were prepared as 20mg/ml solutions in sterile H_2O. The solution was sterilized by filtration through a 0.22µm syringe filter (Millipore).

Synthesis of glycodendrimers and charge of dendrimers: The poly(propylene imine) glycodendrimers of the 5th generation, modified with an open (0.5mPPIg5) and a dense maltose shell (mPPIg5), were prepared by a reductive amination of PPIg5 in the presence of minor (0.5mPPIg5) and excess (mPPIg5) maltose for 0.5mPPIg5 and mPPIg5 as described previously.[22, 23] PPIg4 and PAMAMg5 have a cationic surface charge, whilst the surface charge of 0.5mPPIg5 is also cationic, but less in comparison to PPIg5. In contrast to this, a neutral surface charge is present for the dense shell glycodendrimer mPPIg5.[22, 23, 32] Details on the synthesis and molecular weight determination for mPPIg5-PEG-NH_2, mPPIg4-Tryp, 0.5 mPPIg5-PEG-NH_2 and mPPIg5-SO_3 are available in the Supporting Information.

Molecular modelling of mPPIg5. The 3D structure of the mPPIg5 model which was simulated in explicit water and the radial distribution profiles of selected groups of atoms with respect to dendrimer centre are presented in the Supporting Information as well as simulation methodology.

Cell culture and treatment. N2a cells were kindly donated by Dr. Byron Caughey (Rocky Mountain Laboratories, National Institutes of Health, Hamilton, MT, USA). These were subcloned and infected with the murine adapted scrapie prion strain RML by the method of Bosque and Prusiner (2000).[41] Cell lines were maintained as monolayers at 37°C in 8% CO2 in cultivation media consisting of Dulbecco's Modified Eagle Medium (DMEM)(Gibco) supplemented with 2mM glutamine, 100U/ml penicillin, 100µg/ml streptomycin and 10% heat inactivated foetal bovine serum (FBS)(Gibco). All tissue culture plates used were from Orange Scientific. The medium for all cell lines was replaced every 2-3 days and cells typically reached confluence after 4-5 days at which stage they were split for subculture. For treatment of cells with mPPIg5 and mPPIg5-SO_3, cells were sub-passaged 24 hours prior to treatment at a dilution that allowed cells to be confluent at end of treatment. mPPIg5 and mPPIg5-SO_3 were diluted from stock solutions to 220nM in regular culture media and cells treated for four days. For analysis of PrP^C and PrP^{Sc} content, cells were washed twice with PBS (pH 7.4) and lysed with ice cold lysis buffer (10mM Tris, pH 7.4, 100mM NaCl, 10mM EDTA, 0.5% deoxycholic acid, 0.5% Triton X 100) for 5 min. Cells were detached from plate by pipetting and centrifuged at 1,000 x g for 5mins at room temp to remove cellular debris. Protein concentration of this post-nuclear supernatant was measured by BCA assay (Pierce) according to the manufacturer's instructions. 25µg worth of this lysate was diluted 1/1 with 2X SDS sample buffer and analysed by immunoblot for PrP^C. Protease resistant PrP^{Sc} content of lysed cells was analysed by digesting cellular lysates for 30 min with proteinase K (PK) at a ratio of 250:1 using an amount of 100µg cellular lysate (total protein) per sample. Reactions were stopped by addition of 5mM PMSF. The sample was centrifuged at 16,000g for 30 min, supernatant discarded and pellet re-suspended in 1X SDS sample buffer for immunoblot analysis.

Preparation and Treatment of Brain Homogenates: The mouse prion strains 22A, ME7, 301V and 301C were obtained from the TSE resource Centre and propagated in Tg20 mice (transgenic mice that over express wild-type murine PrP^a).[42] The RML prion strain was obtained through the intracerebral

infection of Tg20 mice with RML infected neuroblastoma cells obtained from Dr. Byron Caughey. Brain homogenate was prepared in PBS (pH 7.4) at 10% (w/v) by successive passing through 18, 20, and 23 gauge needles. Nuclei and tissue debris were removed by centrifugation at 8000 g for 5 min at room temperature. The protein concentration of the homogenate was determined by BCA assay (Pierce). Homogenates were diluted to 1µg/µl in a final concentration of 4% sarkosyl in PBS (pH 7.4) and stored at –80°C.

Treatment of brain homogenates with dendrimers was performed by adding the dendrimer compounds at various concentrations to 25µg of brain homogenate. The final volume was made up to 50µl using 4% sarkosyl in PBS. All Samples were incubated at 37°C for 3 h shaking at 450 rpm. Samples were subsequently subjected to proteolytic digestion with PK at a 1:50 (w/w) ratio. The reaction was stopped with 5 mM PMSF. Samples were centrifuged at 16,000g, supernatant removed and pellet resuspended in 1x SDS PAGE loading buffer.

For studies requiring a low pH, brain homogenate was prepared in sterile dH_2O at 10% (w/v) by successive passing through 18, 20, and 23 gauge needles. Nuclei and tissue debris were removed by centrifugation at 8000 g for 5 min at room temperature. The protein concentration of the homogenate was determined by BCA assay (Pierce). The homogenates were diluted to 2.5µg/µl in dH_2O. 10µl of this (25 µg) was added to 40µl 1.2% IGEPAL CA-630 30mM sodium acetate (pH 2.8) to give a final sample of pH 3.0 or with 1.2% IGEPAL CA-630 40mM Tris acetate (pH 7.4) to give a final sample of pH 7.4. From here on samples were treated identically to those prepared in 4% sarkosyl in PBS except just prior to PK digestion where samples were neutralized by the addition of 50µl of 0.2M Sodium HEPES (pH 7.5) containing 4% sarkosyl.

Immunoblot Analysis and densitometry: Protein samples in 1× SDS sample buffer were incubated for 5 min at 95°C prior to electrophoresis on a 12.5% SDS polyacrylamide gel. After transfer (100 mV, 1 h) to a PVDF membrane (Millipore) and rinsing in TBST (TBS-0.5% Tween 20), unspecific binding sites

were blocked by incubation in 5% dried milk powder (Marvel) in TBST for 1 h, with shaking (250 rpm). The membrane was washed five times in TBST (5 min each, shaking at 250 rpm), and incubated with SAF83 (SPI Bio, diluted to 20ng/mL in TBST) overnight. The membrane was washed 5 times and exposed to goat anti-mouse IgG-ALP secondary antibody (Promega, diluted to 0.1µg/ml in TBST) for 1.5 h, followed by five additional washing steps in TBST (5 min each, shaking at 250 rpm). Blots were developed by exposure to 10mls 5-Bromo-4-chloro-3-indolyl phosphate (BCIP) for 5 min, followed by two washes with dH_2O. Densitometry was performed with the Alphaview Analysis Software. Results were corrected for background by determining the background OD data of two average areas from each gel, and subtracting the average of this from the integral generated for each sample. Brain homogenate from at least two different mice for each prion strain was analyzed. A minimum of three repeats for each sample was performed.

Results

In vitro anti-prion activity of modified dendrimers

To determine the role cationic surface groups play in dendrimer induced reduction of protease resistant PrP^{Sc} (PrP^{res}), neutral maltose dendrimers (mPPI) were modified through the addition of ammonium chloride end-groups on PEG spacers (mPPIg5-PEG-NH_2) or tryptophan end-groups on alkyl spacers (mPPIg4-Tryp). mPPI dendrimers can only interact with PrP^{res} by hydrogen bonding[23] and are not effective against PrP^{res} from 22A prion strain infected brain homogenate *in vitro*.[19] It was speculated that the introduction of cationic end-groups may alter this by enabling electrostatic bonding between the dendrimers and PrP^{res}. To investigate, mPPIg5-PEG-NH2 and mPPIg4-Tryp were incubated with 22A prion strain infected mouse brain homogenates and the protease resistant PrP^{Sc} (PrP^{res}) levels determined by PK digestion, immunoblotting and densitometry (Figure 2). Neither dendrimer was effective at reducing the PrP^{res} content of 22A prion strain infected brain homogenate at the concentrations examined. This demonstrates that introduction of cationic charge to a neutral dendrimer does not necessarily impart *in vitro* anti-prion activity.

The effect of additional cationic surface groups on an already cationic dendrimer was assessed through the use of 0.5 mPPIg5-PEG-NH_2 and a 0.5 mPPIg5 dendrimer modified by the addition of ammonium chloride end-groups on PEG spacer linkages (Figure 1). 0.5mPPIg5 is an open shell glycodendrimer which possesses a cationic charge due to numerous secondary amine groups in its outer shell. The modified version retains this cationic charge as well as an additional six spacered cationic ammonium chloride groups per molecule. To determine if the introduction of these spacered cationic groups improved the anti-prion activity of the dendrimer, 0.5 mPPIg5-PEG-NH_2 was incubated with 22A prion strain infected Tg20 mouse brain homogenate and PrP^{res} levels determined by PK digestion and immunoblotting. Densitometry was performed on the resulting images and the percentage PrP^{res} remaining after dendrimer treatment calculated (Figure 2). 0.5 mPPIg5-PEG-NH_2 proved capable of

reducing the PrP^{res} content of 22A infected brain homogenate but did not exhibit any significant increase in activity over the unmodified form of 0.5 mPPIg5 (Figure 2 and reference 19).

The dendrimers examined up to this point were all cationic dendrimers. To assess the ability of dendrimers with anionic surface groups to reduce PrP^{res} *in vitro*, mPPIg5-SO_3 was utilised. mPPIg5-SO_3 is an anionic dendrimer created through the addition of 1-2 Sulfate groups per maltose molecule in the outer shell of mPPIg5. It's *in vitro* ability to reduce PrP^{res} from 22A prion strain infected brain homogenate was assessed in an identical manner to that already outlined for mPPIg5-PEG-NH_2, mPPIg5-Tryp and 0.5 mPPIg5-PEG-NH_2 (Figure 2). The anionic mPPIg5-SO_3 was effective at reducing PrP^{res} at concentrations as low as 13.6 µM. To our knowledge this is the first demonstration of *in vitro* anti-prion activity for an anionic dendrimer.

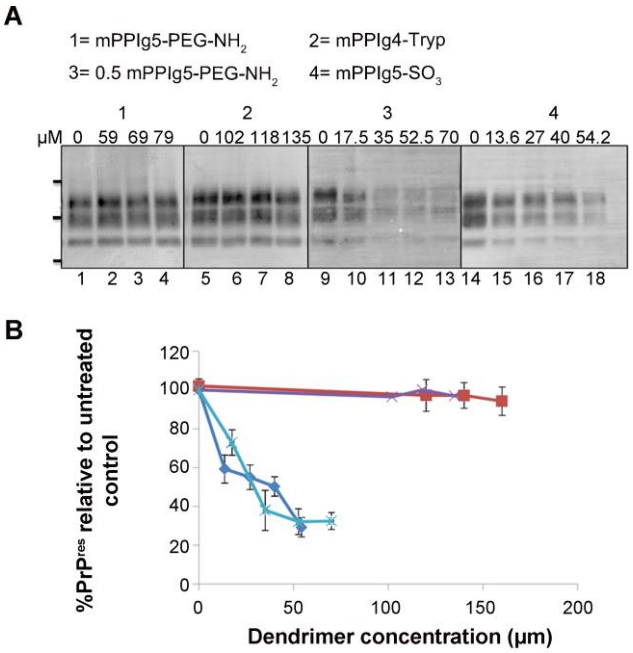

Figure 2 Dendrimer treatment of prion infected brain homogenate. A) 25µg of Tg20 mouse brain homogenates infected with the prion strain 22A were incubated with increasing concentrations of the dendrimer species mPPIg5-PEG-NH_2, mPPIg4-Tryp, 0.5 mPPIg5-PEG-NH_2 and mPPIg5-SO_3. Concentration of dendrimer used for each sample is shown in µM above each lane. Treated samples were digested with PK and analysed by western blot for PrP^{res} with the antibody SAF83. Apparent

molecular mass based on migration of protein standards is indicated for 17, 25, and 30 kDa. **B)** The % PrP^{res} levels remaining following dendrimer treatment and protease digestion, calculated relative to non dendrimer treated controls by densitometry. Legend: mPPIg5-PEG-NH_2; mPPIg4-Tryp; 0.5 mPPIg5-PEG-NH_2; mPPIg5-SO_3. Error bars represent SD; n = 3.

Modified dendrimers activity against prion strains other than 22A

As we and others have demonstrated, the *in vitro* anti-prion activity of dendrimers is prion strain specific.[19-21] To determine if the dendrimers examined here were active against prion strains other than 22A we investigated their activity against 79A, RML, ME7, 301C and 301V prion strains (Figure 3). mPPIg5-SO_3 and 0.5 mPPIg5-PEG-NH_2 exhibited anti-prion activity against the 79A, RML and ME7 prion strain infected brain homogenate. The two dendrimers were more effective in eliminating PrP^{res} from RML and 79A prion strain infected brain homogenate than from 22A and ME7 prion strain infected brain homogenate. Neither dendrimer demonstrated any activity against 301C and 301V prion strains. mPPIg5-PEG-NH_2 and mPPIg4-Tryp, which failed to eliminate PrP^{res} from 22A prion strain infected brain homogenate, did not exhibit activity against any of the prion strains examined.

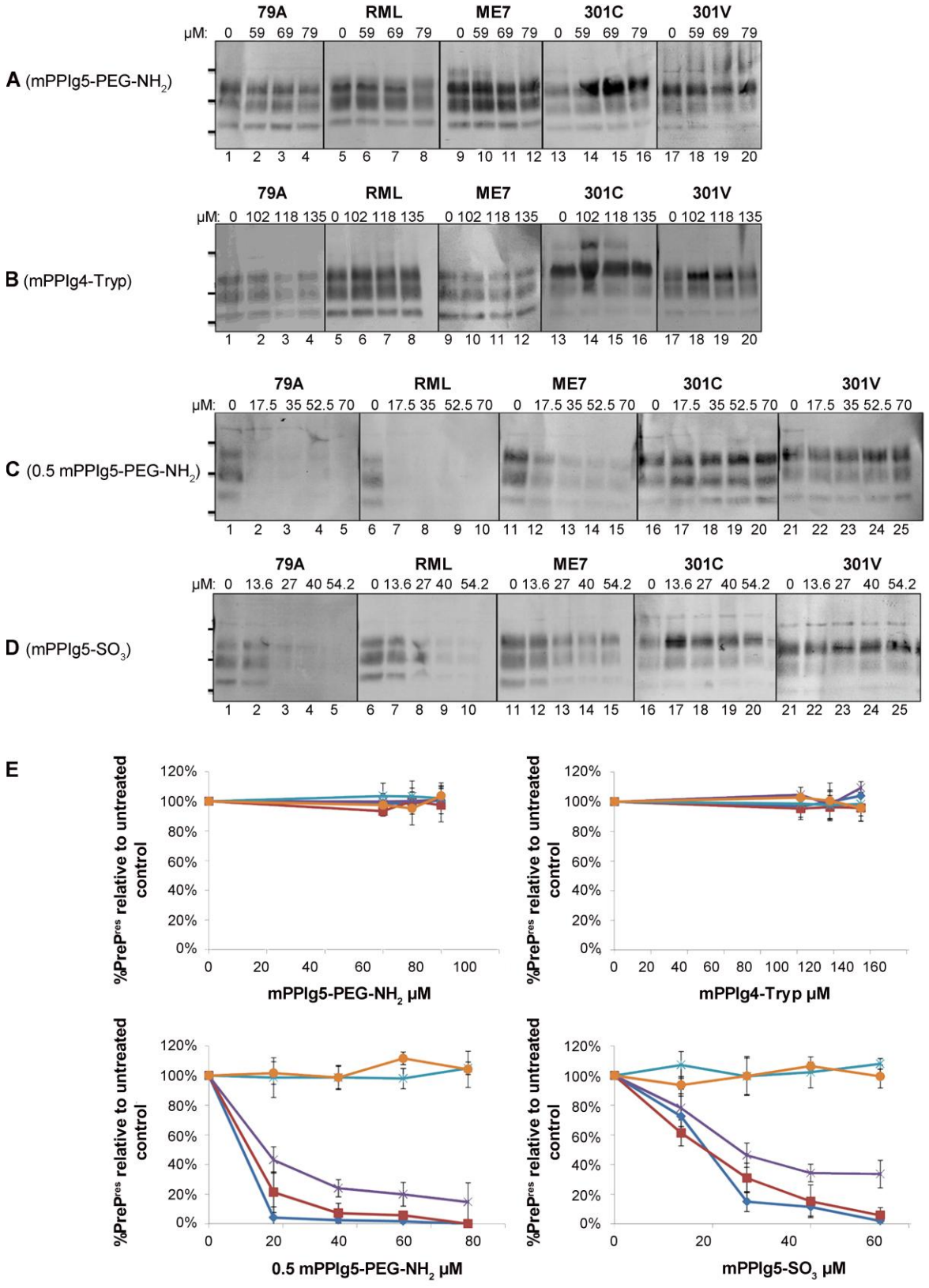

Figure 3 Dendrimer treatment of brain homogenate infected with various prion strains. 25µg of Tg20 mouse brain homogenates infected with the prion strains 79A, RML, ME7, 301C and 301V were incubated with increasing concentrations of the dendrimer species **A)** mPPIg5-PEG-NH_2; **B)** mPPIg4-

Tryp; **C)** 0.5 mPPIg5-PEG-NH_2; and **D)** mPPIg5-SO_3. Samples were subsequently digested with PK and analysed by western blot for PrP^{res} with the antibody SAF83. Apparent molecular mass based on migration of protein standards is indicated for 17, 25, and 30 kDa. **E**) The % PrP^{res} levels remaining following dendrimer treatment and protease digestion were calculated relative to a non dendrimer treated control by densitometry (Legend: 79A; RML; ME7; 301C; 301V). Error bars represent SD; n = 3.

Effect of pH on dendrimers

To our knowledge mPPIg5-SO_3 is the first anionic dendrimer capable of *in vitro* anti-prion activity. This provided the unique opportunity to assess the importance of ionic charge and acidic pH on dendrimer anti-prion activity. Previous studies have demonstrated that the ability of cationic dendrimers to eliminate PrP^{res} from prion infected brain homogenate is optimum at low pH.[20, 21] However it was not possible to deduce if this was due to the increased protonation of cationic dendrimer's amine groups at a low pH resulting in their increased interaction with PrP^{res}[38] or the acidic environment aiding the dendrimer in the denaturation of the PrP^{res} molecule.[21] To examine this, a cationic (PPIg4), anionic (mPPIg5-SO_3) and neutral (mPPIg5) dendrimer were incubated with 22A prion strain infected brain homogenate at a low (pH 3) and neutral pH (pH 7.4) and their ability to reduce PrP^{res} assessed by immunoblot and densitometry (Figure 4). Decreased activity of the anionic dendrimer (mPPIg5-SO_3) at an acidic pH would suggest that it is protonation of cationic groups which is most the important for anti-prion activity. Increased activity of the anionic dendrimer would suggest that the acidic environment aids the dendrimer in the denaturation of the PrP^{res} molecule.

Following incubation with 22A prion strain infected brain homogenate, the cationic (PPIg4) and anionic (mPPIg5-SO_3) dendrimers both exhibited an increased ability to eliminate PrP^{res} at pH3 in comparison to pH7.4. The neutral dendrimer (mPPIg5) was not active against the 22A PrP^{res} at either pH.

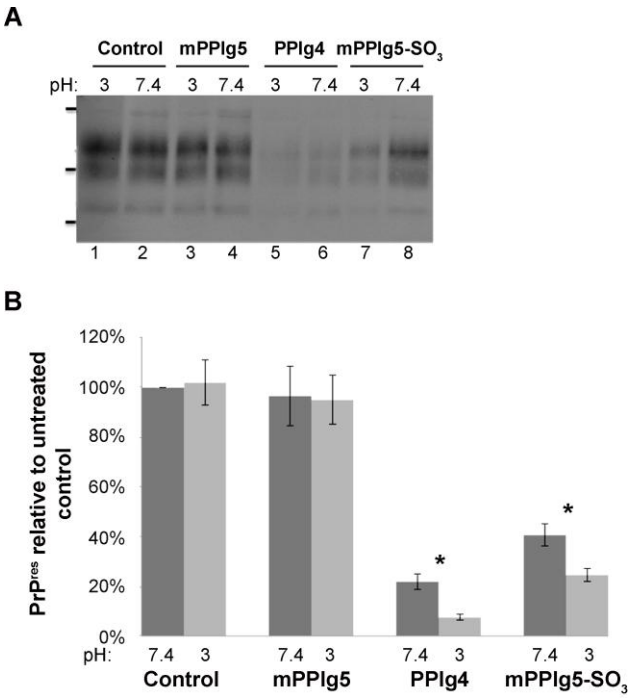

Figure 4 Effect of acidic conditions on dendrimer activity. A) 25µg of Tg20 mouse brain homogenate infected with the 22A prion strain was mock treated (lanes 1 and 2), treated with 72µM mPPIg5 (lanes 3 and 4), treated with 114µM PPIg4 (lanes 5 and 6) or treated with 54.2µM mPPIg5-SO_3 (lanes 7 and 8) at a pH of 3 or 7.4 as indicated. Samples were PK digested and analysed by immunoblot for PrP^{res} with the antibody SAF83. Apparent molecular mass based on migration of protein standards is indicated for 17, 25, and 30 kDa. **B**) Densitometry was performed on the resulting image and % PrP^{res} remaining following treatment with the different dendrimers at pH 7.4 and pH 3 calculated. *Statistically significant difference between treatments at pH 7.4 and pH 3 ($p < 0.05$; analysed using a paired T test with post-hoc analysis by Tukeys test). Error bars represent SD; n = 3.

Intracellular anti-prion activity of mPPIg5-SO_3

The *in vitro* anti-prion effect of the anionic dendrimer mPPIg5-SO_3 was unexpected. To determine if this dendrimer also was capable of eliminating PrP^{res} intracellularly, N2a cells infected with RML prion strain (ScN2a) were incubated with 220nM mPPIg5-SO_3 for four days and PrP^{res} levels determined by PK digestion and immunoblot. For comparison, cells were also treated with 220nM mPPIg5, the unmodified parent of mPPIg5-SO_3 (Figure 5).

In agreement with previous results, mPPIg5 eliminated PrP^{res} from cells after four days of treatment.[23] The anionic mPPIg5-SO_3 did not induce any detectable reduction in PrP^{res} after four days treatment (Figure 5A). Neither treatment had any detectable effect on the level of endogenous PrP^{C} (Figure 5B). In summary, mPPIg5-SO_3 proved capable of eliminating PrP^{res} from the RML prion strain in an *in vitro*, but not an intracellular setting.

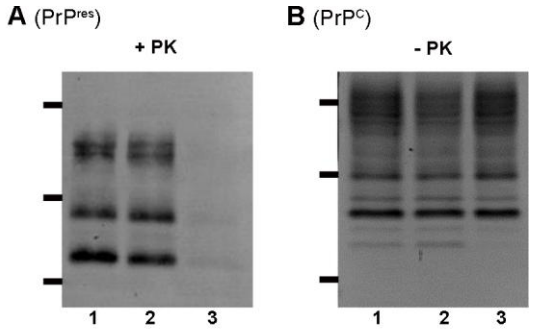

Figure 5 Dendrimer treatment of ScN2a cells. ScN2a cells infected with the RML prion strain were mock treated (lane 1), treated for four days with 220nM mPPIg5-SO_3 (Lane 2), or treated for four days with 220nM mPPIG5 (lane 3). Levels of PrP^{res} were analysed by PK digestion and immunoblot with SAF83 (A). PrP^{C} levels were also analysed to examine the effect of the drugs on PrP^{C} production (B). Apparent molecular mass based on migration of protein standards is indicated for 17, 25, and 30 kDa. n = 3.

Structural characteristics of mPPIg5 obtained from molecular modeling

The aim of this theoretical calculation study was to obtain the 3D structure of mPPIg5 in a water environment and to examine the theoretical backfolding potential of peripheral groups (maltose units) in mPPIg5. In a recently published study,[23] we postulated that mPPIg5 can be considered as a amphiphilic macromolecule, consisting of a cationic core and a neutral surface tailored by the presence of dense maltose shell (Scheme 1A). This working hypothesis is supported by data obtained from polyelectrolyte titration experiments, zetapotential measurements, and streaming potential pH titration.[23]

The 3D model of water solvated mPPIg5 is presented in Figure S15. From this model, the characteristics sizes for radius of gyration (Rg = 21.1 Å) and maximal dendrimer atom distance from the dendrimer

center (Rmax = 33.3 Å) was determined. This model was also used to determine the radial distribution profiles (radial densities) of selected atom groups with respect to the dendrimer center (Figure S16; further details in the Supporting Information). From the radial distribution functions (Figure S16) one can see that the majority of maltose units are located in the outer shell with other maltose molecules located within the PPI scaffold. The maltose molecules in the model which are located deeper within the PPI part of the mPPIg5 dendrimer, were introduced during the process of PPIg5 functionalization (as a consequence of backfolded PPI branches of the primary PPIg5 dendrimer). In reality, some of the deeper backfolded sugars may not be present as the possibility of maltose molecules penetrating deeply into the PPI scaffold is limited. Additionally, the functionalization of the outer PPI branches is a rapid process meaning some of the deeper backfolded sugars may not be present (supported by our previous results from mass spectroscopy)[22,23] Furthermore, the dense nature of the outer sugar shell of mPPIg5 and the presence of numerous hydrogen bonds which "stiffens" this structure, (423 H-bonds in our model) should prevent any large "dynamic" backfolding events

Maltose units backfolded deeply within the PPI scaffold were identified and are visualized in Figure S17. Out of mPPIg5's 128 maltose units, only 9 were determined to be backfolded in our model. Three of these (Figure S17; green residues) were attached to PPI primary amines which were very close to the core. Therefore these 3 molecules are unlikely to be present in the real mPPIg5 macromolecule

The contribution of backfolded maltose units to the surface composition of mPPIg5 is represented in Scheme 1A. We were interested in examining this as the surface composition of a dendrimer is largely responsible for determining its biological activity. Our model demonstrates that mPPIg5's surface is mainly composed of a dense shell of maltose molecules with backfolded units making only a minor contribution (Scheme 1A).

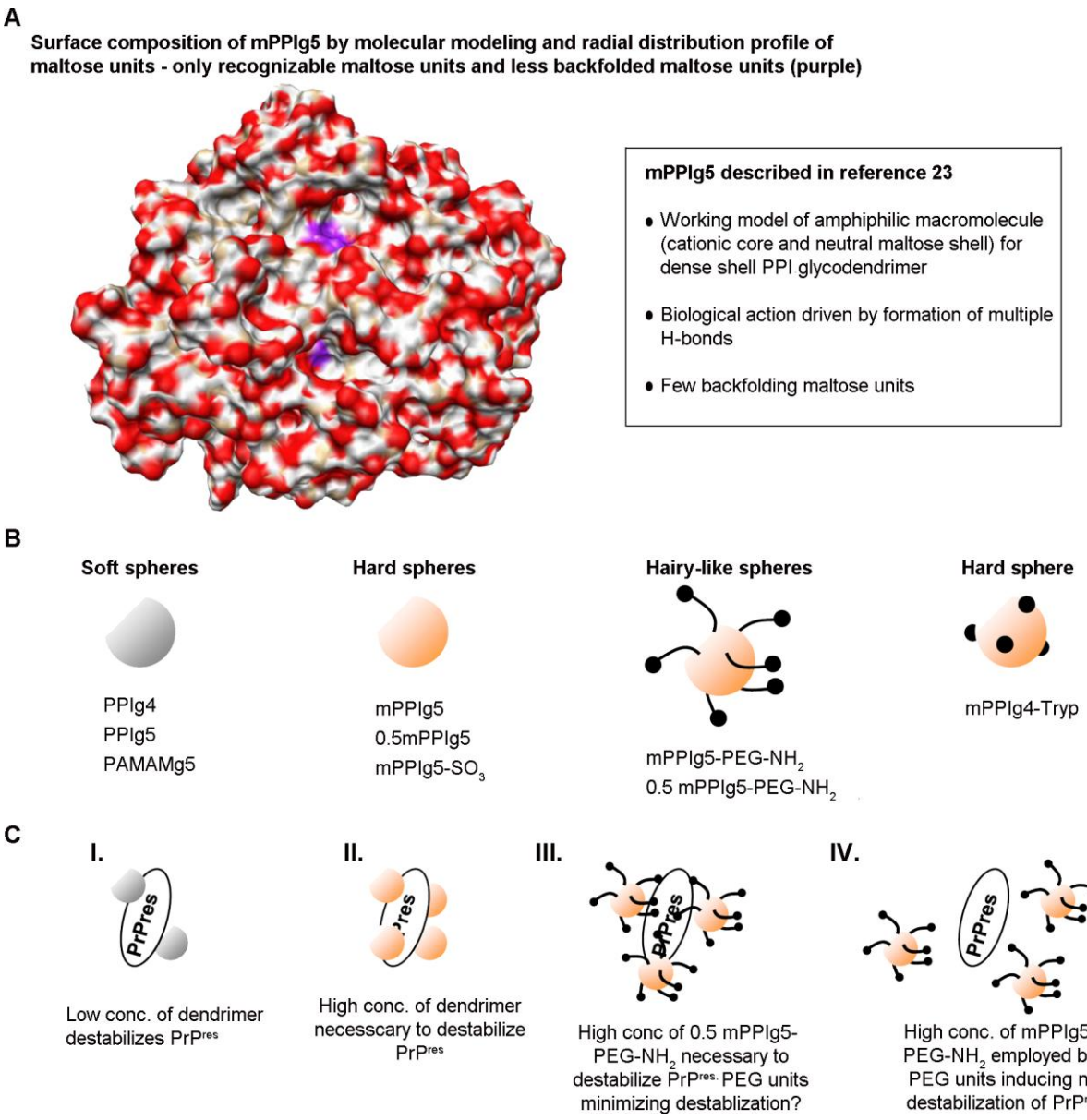

Scheme 1. Glycodendrimer's anti-prion activity in comparison to polyamine dendrimers. A) Surface composition of mPPIg5 determined by molecular modeling and radial distribution profile of maltose units – only recognizable maltose units and less backfolded maltose units (purple) shown. **B**) **Soft spheres:** (highly) flexible spherical-like polyamine dendrimers PPIg4, PPIg5 and PAMAMg5; **Hard spheres:** rigid- and spherical-like glycodendrimers mPPIg5 and mPPIg5-SO_3. Low probability of backfolding. The maltose units in 0.5 mPPIg5 possess a slightly higher probability of backfolding than the maltose units in mPPIg5 and mPPIg5-SO_3; **Hairy-like spheres**: PEGylated pimary amino groups on a 5th generation PPI scaffold can be considered as randomly distributed hairy units in mPPIg5-PEG-NH_2 and 0.5 mPPIg5-PEG-NH_2; **Hard sphere**: alkylated tryptophan units are randomly distributed in the

dense maltose shell of the 4th generation PPI dendrimer mPPIg4-Tryp. **C**) Different interaction features between soft spheres (I.) and hard spheres/hairy-like spheres (II.-IV.): I. (highly) flexible polyamine dendrimers may produce the strongest interactions with PrP^{res} from different prion strains. This is suggested by our results which indicate relatively low concentrations of these dendrimers are needed to render PrP^{res} sensitive to proteases; II. + III. Higher concentrations of these dendrimers were necessary to reduce PrP^{res} from different prion strains. IV. Positive charge of PEGylated primary amino groups had no advantage in promoting mPPIg5-PEG-NH_2's anti-prion activity.

A

Glycodendrimer	Charge of core structure dendrimer	Surface group	Charge of surface groups	Structure of glycodendrimers	Anti-PrP^{res} activity?
mPPIg5-PEG-NH_2	neutral	PEG-$NH_3^+Cl^-$	cationic	DS	✘
mPPIg4-Tryp	neutral	tryptophan	cationic	DS	✘
0.5 mPPIg5-PEG-NH_2	cationic	PEG-$NH_3^+Cl^-$	cationic	OS	✓
mPPIg5-SO_3	neutral	sulphate	anionic	DS	✓

B

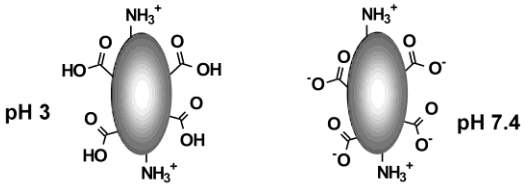

Dendrimer	Surface group	Charge	Chemical interactions possible pH: 3	Chemical interactions possible 7.4	*In vitro* anti-PrP^{res}* activity? pH: 3	*In vitro* anti-PrP^{res}* activity? 7.4	Intracellular anti-PrP^{res}** activity?
mPPIg5	maltose	neutral	H bonds	H bonds	✘	✘	✓
PPIg4	NH_2^-	cationic	H bonds	electrostatic	✓	✓	✓
mPPIg5-SO_3	sulphate	anionic	electrostatic > H bonds	H bonds > electrostatic	✓	✓	✘

Minor interactions at pH 3 and 7.4 = OH-π and others

DS = Dense Shell; OS = Open shell; * Tested against PrP^{res} from 22A infected brain homogenate; ** Tested against ScN2a cells

Scheme 2. Summary of results

A) Summary of anti-prion activity of novel modified dendrimers. mPPIg5-PEG-NH_2 and mPPIg4-Tryp did not demonstrate anti-PrP^{res} activity against any of the prion strains examined. 0.5mPPIg5-PEG-NH_2 and mPPIg5-SO_3 demonstrated an ability to reduce PrP^{res} from 22A, 79A, RML and ME7 prion strain infected mouse brain homogenate.

B) Nature of interactions between dendrimers at pH 3 and pH 7.4. Proteins and dendrimers are more protonated at pH 3 than pH 7.4, influencing the nature of chemical interactions which occur. At pH 3 for example, PrP^{res} must be completely protonated. Thus, electrostatic interactions with cationic dendrimers are rare and hydrogen bonding dominates. The sulfated groups of the anionic glycodendrimer mPPIg5-SO_3 are deprotonated at pH 3 and may undergo electrostatic interactions with protonated amino groups and hydrogen bonding with protonated acids groups. For further information see Supporting information, Fig S14.

Discussion

The *in vitro* anti-prion effect of a dendrimer has always previously been related to its cationic surface charge density. However, we recently demonstrated that maltose modified dendrimers (mPPI) with a neutral surface charge may interact with PrP^{Sc} and PrP peptides and that this interaction must be facilitated through hydrogen bonding.[22, 23] In this study we demonstrate an even more startling result – the ability of an anionic dendrimer (mPPIg5-SO_3) to reduce protease resistant PrP^{Sc} (PrP^{res}) from specific prion strains. How can dendrimers with such polar opposite surface charges interact with the same protein? The phenomena may be explained by the existence of patches of minor surface charge on the PrP^{res} molecule opposite to the major surface charge. This would allow both cationic and anionic dendrimers to electrostatically interact with the PrP^{res} molecule. Evidence for dendrimers interacting with pockets of minor surface charge can be found in a number of previous studies with albumin[43], liver alcohol dehydrogenase[33] and lysozyme protein[44]. Thus it may be concluded that cationic, anionic and neutral dendrimers can all interact with PrP^{res} and neither the net charge of PrP^{res} or the charge of a dendrimer are limiting in determining dendrimer/prion interactions.

It should be noted that the predominant surface charge of PrP^{res} is difficult to determine as the isoelectric point (pI) of PrP^{res} displays a considerable degree of hetrozygozity. PrP^{Sc} aggregates have an average pI of 4.6 making them mostly negatively charged at a neutral pH.[38] Thus in these conditions cationic dendrimers may interact with the predominantly negatively charged groups of the PrP^{res} molecule whilst anionic dendrimers may interact with pockets of cationic charge. To ensure consistency, PrP^{res} was prepared in bulk in buffered solutions (see materials and methods) before aliquots were taken and examined with the various dendrimers.

Whilst we have shown that cationic charge is not necessary for a dendrimers anti-prion activity, dendrimers with a high cationic charge density do appear to be the most potent anti-prion dendrimers.[20, 24, 37] This is presumably due to their superior ability to bind to and/or destabilize the PrP^{res} molecule.

However, cationic charge on its own is not sufficient for a dendrimer to possess anti-prion activity. This is demonstrated by the fact that the modification of neutral glycodendrimers (mPPI) with the cationic groups tryptophan (mPPIg4-Tryp) or ammonium chloride (mPPIg5-PEG-NH_2) did not induce anti-prion activity against any of the prion strains examined (Figure 2 and Figure 3). Too few tryptophan and ammonium chloride groups may have been attached per mPPI molecule and so the cationic charge introduced may have not been sufficient.

An alternative explanation for the lack of anti-prion activity of mPPIg4-Tryp and mPPIg5-PEG-NH_2 is that the cationic groups added to these dendrimers were on spacers and so the dendrimers may lack the necessary surface charge density or structure of molecule required for effective anti-prion activity. In other words, the use of spacers may prevent the necessary density of reactive groups at the dendrimer's surface, inhibiting its interaction with the PrP^{res} molecule. This would also explain how mPPIg5-PEG-NH_2 had no effect on PrP^{res} from RML infected brain homogenate whilst unmodified mPPIg5 (no spacers) was effective.[23] Numerous sources of evidence support the idea that a high surface density of reactive groups is necessary for a dendrimer to effectively interact with and/or destabilize the PrP^{res} molecule. For example the increased anti-prion activity generally displayed by cationic dendrimers in comparison to linear molecules of similar MW and charge has been attributed to the higher density of surface amino groups on the repeatedly branched, highly structured dendrimers.[20] The increased potency of high generation dendrimers over low generation dendrimers also suggests the importance of a high density of surface reactive groups.[20, 21, 23, 37] This relationship between the anti-prion activity of a dendrimer and a high density of reactive surface groups is not limited to cationic dendrimers. The neutral dendrimers mPPIg5 and surface modified PAMAM-OH both possess hydroxyl units at their surface but only mPPIg5 displays anti-prion activity for example.[20, 23] This has been attributed to the high density of hydroxyl units at the surface of mPPIg5 in comparison to PAMAM-OH.[23] As mPPIg5-SO_3 is a modified dense shell dendrimer, this may also explain why an anti-prion effect was observed for this anionic dendrimer when no previous reports of an effective anionic dendrimer exist.

Dendrimer branches are generally capable of back-folding and as a consequence peripheral functional groups may occupy the interior of the dendrimer rather than being present on the surface[45-48]. This is most common in dendrimers with small peripheral groups and a flexible dendritic scaffold. PPIg4, PPIg5 and PAMAMg5 can all be considered relatively flexible molecules (Scheme 1B). In contrast, a recent study suggests that mPPIg5 can be considered as a spherical amphiphilic macromolecule, possessing a neutral surface charge.[23] Theoretical calculations agree with this model and indicate few backfolding maltose units (Scheme 1A and Supporting Information). mPPIg5-SO_3, mPPIg4-Tryp and mPPIg5-PEG-NH_2 are all derived from mPPIg5, thus a similar lack of flexibility can be assumed for these molecules. 0.5mPPIg5 and 0.5mPPIg5-NH_2 will possess peripheral maltose groups capable of back-folding but should maintain a spherical shape. mPPIg5-PEG-NH_2 and 0.5 mPPIg5-PEG-NH_2 may be considered "hairy like spherical units" due to the presence of isolated and randomly distributed peripheral PEGylated primary amine groups. The concept of back-folding for PEGylated primary amine groups is much more significant than back-folding of bulky maltose groups in 0.5mPPIg5 and 0.5mPPIg5-NH_2. The flexibility of a dendrimer may have an effect on its ability to reduce PrP^{res} as dendrimers with a more flexible structure (e.g. PPIg4, PPIg5, PAMAMg5) required a much lower concentration of dendrimer to reduce PrP^{res} than the less flexible gycodendrimers used in this study.[19] This may again be related to the issue of how many surface groups a dendrimer may get in contact with PrP^{res}, flexible dendrimers presumably being more adaptable than rigid dendrimers at this process. Future work in this area should help elucidate the significance of flexibility in dendrimer anti-prion activity.

The *in vitro* anti-prion effect of mPPIg5-SO_3 was prion strain dependent. The prion strains RML and 79A were the most susceptible to mPPIg5-SO_3, followed by 22A and ME7 whilst the prion strains 301C and 301V were completely resistant at the concentrations examined. Remarkably this hierarchy of prion strain susceptibility (79A, RML > 22A, ME7 >>> 301C, 301V) is comparable to that observed for the

cationic dendrimers, PPIg4, PAMAMg5 and 0.5mPPIg5.[19] It is quite surprising that dendrimers of opposite charge would display such a similar hierarchy of prion strain susceptibility. Working on the basis that this is not a simple coincidence, the result suggests two possible scenarios. Firstly, the effect of dendrimers on PrP^{res} is governed by the ability of a dendrimer to bind to PrP^{res}. In this scenario prion strains such as 301C and 301V, which were resistant to all the species of dendrimers examined, would have to possess insufficient binding sites on their surface for each of the different dendrimers examined to explain their resistance. We and others have shown that dendrimers can interact with PrP^{res} through pockets of minor surface charge, hydrogen bonds[22, 23] and hydrophobic interactions,[25] hence the existence of a prion strain which displays none of these features seems unlikely. Alternatively, a dendrimers ability to bind PrP^{res} from various strains may be somewhat ubiquitous, and it is the subsequent ability of PrP^{res} from different strains to resist the destabilizing effects induced by a particular dendrimer that is important. In this scenario various dendrimers would bind to PrP^{res} from different prion strains through a variety of mechanisms such as electrostatic interactions and hydrogen bonding (Scheme 2B). The type of binding would be dependent on the species of dendrimer but the ability of PrP^{res} to resist the destabilizing effects induced by a particular dendrimer would vary according to the prion strain.

The results from this study confirm that the cationic dendrimer, PPIg4, is most efficient at an acidic pH. The results also demonstrate that the anionic dendrimer, mPPIg5-SO_3, is most effective at an acidic pH (Figure 4). This demonstrates that "hyper charging" of cationic groups on dendrimers cannot be the sole explanation for a dendrimers increased activity at a low pH. The results instead suggest that an acidic pH aids dendrimers in the destabilization of the PrP^{res} molecule. This destabilization appears subtle, and not to an extent where prion strains are directly made more susceptible to PK digestion. However the slight destabilization/change in conformation that does occur may enable dendrimers to interact more efficiently with PrP^{res} and so dendrimer induced denaturation of PrP^{res} is increased. Acidic pH may therefore aid any dendrimer that can induce denaturation of a prion strain, regardless of its charge

(Scheme 2B). An alternative interpretation for these results relates to the structure of PPIg4 and mPPIg5-SO_3 at low pH. It has been proposed that an acidic pH may promote an extended conformation of dendrimer, which in turn may facilitate more efficient interaction with PrP^{res}.[49] PPIg4 is considered a highly flexible dendrimer with backfolded peripheral amino groups.[50] Acidic pH does not negatively influence the flexibility of PPIg4 and so an increased interaction with PrP^{res} is theoretically possible. However it is unlikely that acidic pH has a similar effect on mPPIg5-SO_3. Polyelectrolyte titration experiments with mPPIg5 have indicated that the maltose units of this molecule are unlikely to be capable of back-folding at pH 5.5.[23] Thus one can assume a similar lack of flexibility for the maltose units in mPPIg5-SO_3. Furthermore, zeta potential measurements of mPPIg5-SO_3 reveal an anionic surface charge at pH 3 (Supporting information, Fig S14). This implies the presence of anionic sulfate groups in the outer shell of mPPIg5-SO_3 which would hamper the back-folding ability of the peripheral units, reducing the flexibility of the molecule.

It is worth nothing that the predominant chemical interactions which occur between PrP^{res} and cationic and anionic dendrimers at an acidic pH are quite different to those that occur at a neutral pH (Scheme 2B). For instance, cationic dendrimers will be largely limited to hydrogen bonding at pH 3 (Scheme 2B). Yet despite these alterations, both the cationic and anionic dendrimer used in this study retained their ability to reduce PrP^{res} from the 22A prion strain at a low pH (Figure 4). This again suggests that the mechanism by which a dendrimer binds to PrP^{res} is less important than the ability of the dendrimer to destabilize PrP^{res} from a particular strain following the initial binding.

Despite its *in vitro* effectiveness, mPPIg5-SO_3 was not capable of curing RML infected N2a cells (ScN2a). A previous study employing anionic PAMAM has demonstrated that this anionic dendrimer also lacks intracellular anti-prion activity (the *in vitro* anti-prion ability of anionic PAMAM was not assessed).[51] There are a number of possible explanations for the lack of intracellular activity of these anionic dendrimers. mPPIg5-SO_3 may not be capable of accessing cells and so only works in an *in vitro*

setting where PrP^{res} is readily exposed. Negatively charged dendrimers generally have a poor ability to interact with biological membranes, resulting in poor cell penetration and uptake.[49] However some negatively charged dendrimers do enter cells. Anionic PAMAM dendrimers for example enter the cell by energy dependent, fluid phase endocytosis.[52] mPPIg5-SO_3 and anionic PAMAM dendrimers are quite different in structure and size so it is possible that the high MW sulfated mPPIg5-SO_3 cannot enter cells or is not processed in a manner that permits it to come into contact with the prion protein. Alternatively, the anionic mPPIg5-SO_3 may be ineffective in the harsh environment of late endosomes/lysosomes where dendrimers are believed to interact with and eliminate PrP^{Sc}. However, results from this study which show that mPPIg5-SO_3 was most effective at an acidic pH do not support this hypothesis. Finally, there is speculation that dendrimers may eliminate PrP^{Sc} from cells by inhibiting the conversion of PrP^{C} to PrP^{Sc}.[38, 51] Cationic dendrimers may be more effective than the anionic mPPIg5-SO_3 in inducing the changes in PrP^{Sc} structure or processing potentially necessary to achieve this effect.

In conclusion, the data from this and other studies allowed us to develop the following working model for a dendrimers *in vitro* method of action:

Specific dendrimers bind preferentially to the PrP^{res} protein as this aberrantly folded isoform has many binding sites available.[25] The surface and structural patchiness of proteins and the possibility of hydrogen bonding ensure that not just cationic dendrimers bind to PrP^{res}. Specific anionic and neutral dendrimers are also capable of binding PrP^{res} (Scheme 1C and 2B). However the binding of dendrimers is in itself not sufficient for PrP^{res} to be rendered protease sensitive. Instead, once bound the dendrimers begin to destabilize the PrP^{res} molecules (Scheme 1C), presumably through a mechanism somewhat independent of a dendrimer's specific charge such as by acting as water structure perturbing solutes. Certain prion strains may be particularly resistant to this destabilizing effect, thus explaining the prion strain dependent effect of dendrimers. Other strains will be highly susceptible and be rendered protease sensitive. This is most likely due to alterations in their β sheet secondary structure (Scheme 1C). In

general, a dendrimer with a high density of surface reactive groups will be most efficient in destabilizing PrP^{res} *in vitro*. The surface groups may be cationic, anionic or neutral in charge as long as a high surface density of these groups is present.

Future work should focus on the more speculative aspects of this model such as the relationship between a dendrimers ability to bind to PrP^{res} and its ability to destabilize that same molecule and determining what features of PrP^{res} define its protease resistance – a question dendrimers are particularly well poised to address.

Conclusion

This study suggests that dendrimers eliminate PrP^{res} by destabilizing the molecule and rendering it susceptible to proteolysis. This ability is not dependent on any particular charge of dendrimer but does require a high density of reactive surface groups on the dendrimer. By understanding what makes a dendrimer an effective *in vitro* anti-prion drug, design of more effective dendrimers for therapeutic use will be possible.

Abbreviations

22A, 79A, RML, ME7, 301C, 301V = mouse adapted prion strains; 0.5mPPI = maltose modified PPI with an open maltose shell; 0.5mPPIg5-PEG-NH2 = 5th generation 0.5mPPI with NH3+Cl- endgroups on a PEG spacer; mPPI = maltose modified PPI; mPPI-PEG-NH2 = 5th generation mPPI with NH3+Cl- endgroups on a PEG spacer; mPPIg5-SO_3 = 5th generation mPPI modified with SO_3^- end groups; mPPIg4-Tryp = 4th generation mPPI with Tryptophan endgroups on alkyl spacers; PK = proteinase K; PPI = poly(amido amine); PrP^C = normal isoform of prion protein; PrP^{res} = protease resistant form of PrP^{Sc}; PrP^{Sc} = disease associated isoform of prion protein.

Acknowledgments

This work was supported by funding from University College Dublin, the Irish Research Council for Science, Engineering & Technology (IRCSET) the European Union (Dendrimers in Biomedical Applications - COST TD0802, Neuroprion - FOOD-CT-2004-506579), The Irish Department of Agriculture, Food and Rural Development (FIRM 01-R&D-D-160), The Czech national Cost project OC10053, Swiss project "POLYDEN" financed by SER (2012-2013) in the COST framework, The Saxon Ministry for Science and Art and The German Ministry for Education and Science. The authors thank Dr. S. Schwarz (IPF Dresden) for technical support in zeta potential measurement.

Corresponding Authors

* Dr. James M. McCarthy, School of Biology and Environmental Science, University College Dublin, Belfield, Dublin 4, Ireland. E-mail: jim.mccarthy@ucd.ie

*Dr. Dietmar Appelhans, Leibniz Institute of Polymer Research Dresden, Hohe Strasse 6, D-01069 Dresden (Germany). E-mail: applhans@ipfdd.de

Author Contributions

The manuscript was written through contributions of all authors. All authors have given approval to the final version of the manuscript.

References

(1) Hsiao, K. K.; Groth, D.; Scott, M.; Yang, S. L.; Serban, H.; Rapp, D.; Foster, D.; Torchia, M.; Dearmond, S. J.; Prusiner, S. B. *Proc. Natl. Acad. Sci. U. S. A.* **1994,** *91*, 9126-30.

(2) Telling, G. C.; Parchi, P.; DeArmond, S. J.; Cortelli, P.; Montagna, P.; Gabizon, R.; Mastrianni, J.; Lugaresi, E.; Gambetti, P.; Prusiner, S. B. *Science* **1996,** *274*, 2079-82.

(3) Safar, J.; Wille, H.; Itri, V.; Groth, D.; Serban, H.; Torchia, M.; Cohen, F. E.; Prusiner, S. B. *Nat. Med.* **1998,** *4*, 1157-65.

(4) Gambetti, P.; Dong, Z.; Yuan, J.; Xiao, X.; Zheng, M.; Alshekhlee, A.; Castellani, R.; Cohen, M.; Barria, M. A.; Gonzalez-Romero, D.; Belay, E. D.; Schonberger, L. B.; Marder, K.; Harris, C.; Burke, J. R.; Montine, T.; Wisniewski, T.; Dickson, D. W.; Soto, C.; Hulette, C. M.; Mastrianni, J. A.; Kong, Q.; Zou, W. Q. *Ann. Neurol.* **2008,** *63*, 697-708.

(5) Colby, D. W.; Wain, R.; Baskakov, I. V.; Legname, G.; Palmer, C. G.; Nguyen, H. O.; Lemus, A.; Cohen, F. E.; DeArmond, S. J.; Prusiner, S. B. *PLoS Pathog* **2010,** *6*, e1000736.

(6) Prusiner, S. B. *Science* **1982,** *216*, 136-44.

(7) Prusiner, S. B. *Proc. Natl. Acad. Sci. U. S. A.* **1998,** *95*, 13363-83.

(8) Kim, J. I.; Cali, I.; Surewicz, K.; Kong, Q.; Raymond, G. J.; Atarashi, R.; Race, B.; Qing, L.; Gambetti, P.; Caughey, B.; Surewicz, W. K. *J. Biol. Chem.* **2010,** *285*, 14083-7.

(9) Wang, F.; Wang, X.; Yuan, C. G.; Ma, J. *Science* **2010,** *327*, 1132-5.

(10) Bruce, M. E.; Fraser, H. *Curr. Top. Microbiol. Immunol.* **1991,** *172*, 125-38.

(11) Fraser, H.; Dickinson, A. G. *J. Comp. Pathol.* **1973,** *83*, 29-40.

(12) Bruce, M. E. *Br. Med. Bull.* **1993,** *49*, 822-38.

(13) Bruce, M. E.; McBride, P. A.; Farquhar, C. F. *Neurosci. Lett.* **1989,** *102*, 1-6.

(14) Colby, D. W.; Prusiner, S. B. *Cold Spring Harb Perspect Biol* **2011,** *3*, a006833.

(15) Bessen, R.; Marsh, R. *J. Virol.* **1994,** *68*, 7859-68.

(16) Prusiner, S. B. *Science* **1991,** *252*, 1515-22.

(17) Hecker, R.; Taraboulos, A.; Scott, M.; Pan, K.; Yang, S.; Torchia, M.; Jendroska, K.; DeArmond, S.; Prusiner, S. *Genes Dev.* **1992,** *6*, 1213-1228.

(18) Deleault, N. R.; Kascsak, R.; Geoghegan, J. C.; Supattapone, S. *Biochemistry (Mosc).* **2010,** *49*, 3928-3934.

(19) McCarthy, J. M.; Rasines Moreno, B.; Appelhans, D.; Rogers, M. *Adv. Healthcare Mater* **2012,** *1,* 768-772.

(20) Supattapone, S.; Nguyen, H. O.; Cohen, F. E.; Prusiner, S. B.; Scott, M. R. *Proc. Natl. Acad. Sci. U. S. A.* **1999,** *96*, 14529-34.

(21) Supattapone, S.; Wille, H.; Uyechi, L.; Safar, J.; Tremblay, P.; Szoka, F. C.; Cohen, F. E.; Prusiner, S. B.; Scott, M. R. *J. Virol.* **2001,** *75*, 3453-61.

(22) Klajnert, B.; Appelhans, D.; Komber, H.; Morgner, N.; Schwarz, S.; Richter, S.; Brutschy, B.; Ionov, M.; Tonkikh, A. K.; Bryszewska, M. *Chem. Eur. J.* **2008,** *14*, 7030-7041.

(23) Fischer, M.; Appelhans, D.; Schwarz, S.; Klajnert, B.; Bryszewska, M.; Voit, B.; Rogers, M. *Biomacromolecules* **2010,** *11*, 1314-1325.

(24) Solassol, J.; Crozet, C.; Perrier, V.; Leclaire, J.; Beranger, F.; Caminade, A.; Meunier, B.; Dormont, D.; Majoral, J.; Lehmann, S. *J. Gen. Virol.* **2004,** *85*, 1791-9.

(25) Lane, A. R.; Stanley, C. J.; Wilson, S. M. Binding of pathological forms of prion proteins. U.S. Patent 7,659,076 B2, February 9, 2010.

(26) Goedert, M.; Spillantini, M.; Jakes, R.; Rutherford, D.; Crowther, R. *Neuron* **1989,** *3*, 519-526.

(27) Vermersch, P.; Delacourte, A.; Javoy-Agid, F.; Hauw, J. J.; Agid, Y. *Ann. Neurol.* **1993,** *33*, 445-450.

(28) Poorkaj, P.; Bird, T. D.; Wijsman, E.; Nemens, E.; Garruto, R. M.; Anderson, L.; Andreadis, A.; Wiederholt, W. C.; Raskind, M.; Schellenberg, G. D. *Ann. Neurol.* **1998,** *43*, 815-825.

(29) Lee, V. M.; Goedert, M.; Trojanowski, J. Q. *Annu. Rev. Neurosci.* **2001,** *24*, 1121-59.

(30) Klajnert, B.; Cortijo-Arellano, M.; Bryszewska, M.; Cladera, J. *Biochem. Biophys. Res. Commun.* **2006,** *339*, 577-582.

(31) Wasiak, T.; Ionov, M.; Nieznanski, K.; Nieznanska, H.; Klementieva, O.; Granell, M.; Cladera, J.; Majoral, J.-P.; Caminade, A. M.; Klajnert, B. *Mol Pharm* **2011,** *9*, 458–469.

(32) Klementieva, O.; Benseny-Cases, N.; Gella, A.; Appelhans, D.; Voit, B.; Cladera, J. *Biomacromolecules* **2011,** *12*, 3903-3909.

(33) Gabellieri, E.; Strambini, G. B.; Shcharbin, D.; Klajnert, B.; Bryszewska, M. *Biochimica et Biophysica Acta (BBA)-Proteins & Proteomics* **2006,** *1764*, 1750-1756.

(34) Klajnert, B.; Stanisławska, L.; Bryszewska, M.; Pałecz, B. *Biochimica et Biophysica Acta - Proteins and Proteomics* **2003,** *1648*, 115-126.

(35) Klajnert, B.; Sadowska, M.; Bryszewska, M. *Bioelectrochemistry* **2004,** *65*, 23-26.

(36) Solassol, J.; Arlotto, M.; Lehmann, S. *J. Hosp. Infect.* **2004,** *57*, 156-161.

(37) Cordes, H.; Boas, U.; Olsen, P.; Heegaard, P. *Biomacromolecules* **2007,** *8*, 3578-3583.

(38) Lim, Y.; Mays, C.; Kim, Y.; Titlow, W.; Ryou, C. *Biomaterials* **2010,** *31*, 2025-33.

(39) Boas, U.; Christensen, J. B.; Heegaard, P. M. H. *Dendrimers in medicine and biotechnology: new molecular tools*. Royal Society of Chemistry: Cambridge, U.K., 2006; p 182.

(40) Sebestik, J.; Niederhafner, P.; Jezek, J. *Amino Acids* **2010,** *40*, 301-70.

(41) Bosque, P. J.; Prusiner, S. B. *J. Virol.* **2000,** *74*, 4377-4386.

(42) Fischer, M.; Rulicke, T.; Raeber, A.; Sailer, A.; Moser, M.; Oesch, B.; Brandner, S.; Aguzzi, A.; Weissmann, C. *EMBO J.* **1996,** *15*, 1255-64.

(43) Shcharbin, D.; Klajnert, B.; Bryszewska, M. *J. Biomater. Sci. Polym. Ed.* **2005,** *16*, 1081-1093.

(44) Ciolkowski, M.; Palecz, B.; Appelhans, D.; Voit, B.; Klajnert, B.; Bryszewska, M. *Colloids Surf B Biointerfaces* **2012,** *95*, 103-108.

(45) Mansfield, M. L.; Klushin, L. I. *Macromolecules* **1993,** *26*, 4262-4268.

(46) Scherrenberg, R.; Coussens, B.; van Vliet, P.; Edouard, G.; Brackman, J.; de Brabander, E.; Mortensen, K. *Macromolecules* **1998,** *31*, 456-461.

(47) Maiti, P. K.; Cagin, T.; Wang, G.; Goddard III, W. A. *Macromolecules* **2004,** *37*, 6236-6254.

(48) Kłos, J.; Sommer, J. U. *Macromolecules* **2009,** *42*, 4878-4886.

(49) Heegaard, P.; Boas, U.; Otzen, D. *Macromolecular bioscience* **2007,** *7*, 1047-1059.

(50) Ballauff, M.; Likos, C. N. *Angewandte Chemie International Edition* **2004,** *43*, 2998-3020.

(51) Ghaemmaghami, S.; Ullman, J.; Ahn, M.; St Martin, S.; Prusiner, S. *J. Biol. Chem.* **2009,** *285*, 10415-10423.

(52) Perumal, O. P.; Inapagolla, R.; Kannan, S.; Kannan, R. M. *Biomaterials* **2008,** *29*, 3469-76.

Supporting Information

SUPPORTING INFORMATION

Influence of Surface Groups on Poly(propylene imine) Dendrimers Anti-prion Activity

James M. McCarthy[1], Beatriz Rasines Moreno [2], Damien Filippini[2], Hartmut Komber[2], Marek Maly[3,4], Michaela Cernescu[5], Bernhard Brutschy[5], Dietmar Appelhans[2]*, Mark S. Rogers[1].*

[1] School of Biology and Environmental Science,

University College Dublin, Belfield, Dublin 4, Ireland.

[2] Leibniz Institute of Polymer Research Dresden, Hohe Str. 6, 01069 Dresden, Germany.

[3] J. E. Purkinje University, Ceske mladeze 8, 400 96 Usti nad Labem, Czech Republic.

[4] University of Applied Science of Southern Switzerland, Lab Appl Math & Phys LAMFI, CH-6928 Manno, Switzerland.

[5] Institute of Physical and Theoretical Chemistry, Johann-Wolfgang-Goethe University,

Max-von-Laue-Str. 7, D-60438 Frankfurt/Main, Germany.

* Corresponding authors: Dr. James M. McCarthy, School of Biology and Environmental Science, University College Dublin, Belfield, Dublin 4, Ireland. E-mail: jim.mccarthy@ucd.ie

Dr. Dietmar Appelhans, Leibniz Institute of Polymer Research Dresden, Hohe Strasse 6, D-01069 Dresden (Germany). E-mail: applhans@ipfdd.de

Table of Contents for Supporting Information

		page
1	**Methods**	4
	NMR spectroscopy	4
	Mass spectrometry	4
	Determination of electrokinetic properties – zeta potential	4
2	**Synthetic pathways of glycodendrimers mPPIg4-Tryp, 0.5 mPPIg5-PEG-NH_2, mPPIg5-PEG-NH_2 and mPPIg5-SO_3**	5
	Figure S1. Synthetic pathways of glycodendrimers used in this study: (A) mPPIg4-Tryp; (B) mPPIg5-PEG-NH_2 and 0.5 mPPIg5-PEG-NH_2; (C) mPPIg5-SO_3.	5
3	**Molecular weight of compounds used in this study**	8
	Table S1. Molecular weights (M_w) of PPI glycodendrimers mPPIg5-(PEG-NH_2), 0.5 mPPIg5-(PEG-NH_2), mPPIg4-Tryp and PPIg5-SO_3 based on theoretical calculations for their precursors. M_w determined by LILBID-MS.	8
4	**Synthesis of 0.5 mPPIg5-PEG-NH_2**	9
	Synthesis of the precursor PPIg5-PEG-NHBoc (Figure S1)	9
	Synthesis of the precursor 0.5 mPPIg5-PEG-NHBoc (Figure S1)	9
	Synthesis of the precursor 0.5 mPPIg5-PEG-NH_2 (Figure S1)	10
5	**Synthesis of mPPIg5-PEG-NH_2**	11
	Synthesis of the precursor mPPIg5-PEG-NHBoc (Figure S1)	11
	Synthesis of the precursor mPPIg5-PEG-NH_2 (Figure S1)	11
6	**Synthesis of mPPIg5-SO_3**	12
7	**Synthesis of mPPIg4-Tryp**	13
	Synthesis of C10-Tryp (Figure S1)	13
	Synthesis of the precursor PPIg4-Tryp (Figure S1)	14
	Synthesis of mPPIg4-Tryp (Figure S1)	14
8	**NMR spectra of mPPIg4 and mPPIg5**	16
	Figure S2. ^{13}C NMR spectrum of mPPIg5 with dense maltose shell in D_2O.	16
	Figure S3. (A) ^{1}H and (B) ^{13}C NMR spectrum of PPIg4 in D_2O.	17
	Figure S4. ^{13}C NMR spectrum of mPPIg4 in D_2O with signal assignment.	18
	Figure S5. ^{1}H NMR spectra of (A) mPPIg4 and (B) mPPIg5 in D_2O.	19
9	**^{1}H NMR spectra of HO_2C-PEG-NHBoc**	20
	Figure S6. ^{1}H NMR of HO_2C-PEG-NHBoc in DMSO-d6; Used as precursor for synthesizing PPI glycodendrimers mPPIg5-PEG-NH_2 and 0.5 mPPIg5-PEG-NH_2.	20
10	**NMR spectra of PPIg5-PEG-NHBoc and Degree of substitution of PEG unit (HO_2C-PEG-NHBoc) on PPIg5 surface**	21
	Figure S7. ^{1}H NMR of PPIg5-PEG-NHBoc in DMSO-d6; Used as precursor for synthesizing PPI glycodendrimers mPPIg5-PEG-NH_2 and 0.5 mPPIg5-PEG-NH_2. Assignment of a-q for 5th generation PPI scaffold is presented in Figure S2.	21
11	**NMR spectra of 0.5 mPPIg5-PEG-NHBoc**	
	Figure S8. (A) ^{1}H and (B) ^{13}C NMR spectrum of 0.5 mPPIg5-PEG-NHBoc in D_2O. * indicates not assignable ^{13}C NMR signal. Assignment for 1-6 and 1´-6´ (maltose	23

unit as R^2) is presented in Figure S2. Assignment of a-q for 5th generation PPI scaffold is presented in Figure S2.

12 NMR spectra of 0.5 mPPIg5-PEG-NH_2 24

Figure S9. (A) ^1H and (B) ^{13}C NMR spectrum of 0.5 mPPIg5-PEG-NH_2 in D_2O. Assignment for 1-6 and 1´-6´ (maltose unit as R^2) is presented in Figure S2. Assignment of a-q for 5th generation PPI scaffold is presented in Figure S2. 24

13 NMR spectra of C10-Tryp, PPIg4-Tryp and mPPIg4-Tryp 25

Figure S10. ^1H NMR spectrum of methyl ester of C10-Tryp in DMSO-d6. 25

Figure S11. (A) ^1H and (B) ^{13}C NMR spectrum of C10-Tryp-COOH in DMSO-d6. 26

Figure S12. (A) ^1H and (B) ^{13}C NMR spectrum of PPIg4-Tryp in DMSO-d6 27

Figure S13. (A) ^1H NMR spectrum of mPPIg4-Tryp in D_2O. Assignment of 1-6 and 1´-6´ (maltose unit as R^2) is presented in Figure S4. Assignment of a-n for 4th generation PPI scaffold is presented in Figure X-SI. Assignment of l´-n´is presented in Figure S4. 28

14 pH-dependent zeta-potential of mPPIg5-SO_3 29

Figure S14. pH-dependent zeta-potential of mPPIg5-SO_3 possessing no isoelectronic point. The macromolecule is deprotonated and anionic over the measured pH range due to the presence of strong acid substituents in the maltose shell of mPPIg5-SO_3. 29

15 Molecular modeling of the mPPIg5 dendrimer 30

Methods 30

16 Structural characteristics of mPPIg5 dendrimer obtained from molecular modeling 31

Figure S15. Overall structure of simulated mPPIg5 dendrimer presented as stick model (oxygens - red, nitrogens – blue, carbons – beige, hydrogens - white). 31

Figure S16 Radial distribution function of all dendrimer atoms (in black): PPI scaffold (in blue), maltose atoms (in red), only the terminal glucose units of the maltose units atoms (in pink), water (in cyan), and PPI terminal nitrogens (in grey, here the density is multiplied by 100) with respect to two central carbon atoms from the dendrimer core. 31

Figure S17. Visual representation of the terminal glucose rings (stick) of maltose which have at least one atom less than 10 Å from the central carbon (coloured in magenta) of PPI. Glucose rings coloured in green belong to maltose molecules which have at least one atom of their starting part (belonging to the open glucose ring (orange) attached to PPI scaffold) closer than 5 Å from the central carbon atom. PPI structure is represented by a wire background. Dendrimer core is in ball & stick representation. Both central carbons used for RDF are in magenta. 33

17 References 34

1 Methods

NMR Spectroscopy

The NMR measurements were performed using a Bruker Avance III 500 NMR spectrometer operating at 500.13 MHz for ^{1}H and at 125.75 MHz for ^{13}C. The solvent was used as lock and internal standard (DMSO-d_6: δ (^{1}H) = 2.50 ppm, δ (^{13}C) = 39.6 ppm). Spectra recorded from D_2O solutions were referenced on external sodium 3-(trimethylsilyl)-3,3,2,2 tetradeuteropropionate in D_2O (δ (^{1}H) = 0 ppm, δ (^{13}C) = 0 ppm). The signal assignments were confirmed by ^{1}H-^{1}H COSY, ^{1}H-^{1}H TOCSY, ^{1}H-^{13}C HMQC, and ^{1}H-^{13}C HMBC 2D NMR experiments using the standard pulse sequences provided by Bruker.

Mass spectrometry

Laser-induced liquid bead ionization/desorption mass spectrometry (LILBID-MS) is a recently developed method for the soft mass spectrometric investigation of biomolecules and biomolecular complexes.[1] Liquid micro droplets of the aqueous fluid sample (~50 µm) are irradiated by synchronized IR laser pulses (λ = 3 µm) generated by a home built optical parametric oscillator (OPO) based on a $LiNbO_3$ crystal and pumped by a commercial pulsed Nd-YAG laser. The laser energy is absorbed by o-H stretch vibrations of water molecules, which leads to the superexcitation and subsequent explosive disruption of the droplet. The biomolecules ejected into vacuum were analysed by a TOF mass spectrometer. The dendrimer samples were prepared in aqueous solution at concentrations of 4 x 10^{-6} M. All measurements were performed in anionic mode.

Determination of electrokinetic properties – zeta potential

Zetasizer Nano (Malvern Instruments/UK) was used for the determination of the electrokinetic properties of mPPIg5-SO_3. The zetasizer was equipped with a 633 nm He/Ne laser and a non-invasive back scatter (NIBS®) technology. The zetasizer was also used for electrophoretic experiments to determine the electrophoretic velocity of mPPIg5-SO_3 at different pH values. The complex velocity in an electric field, using 120 V/cm, was measured by laser Doppler anemometry employing the He/Ne laser. The apparent electrokinetic potential (zeta-potential, ζ) values were calculated from the complex velocity according to the Smoluchowski equation (M. Smoluchowski in Handbuch der Elektrizität und des Magnetismus Vol II, p 366, Barth, Leipzig, 1921).

2 Synthetic pathways of glycodendrimers mPPIg4-Tryp, 0.5 mPPIg5-PEG-NH_2, mPPIg5-PEG-NH_2 and mPPIg5-SO_3

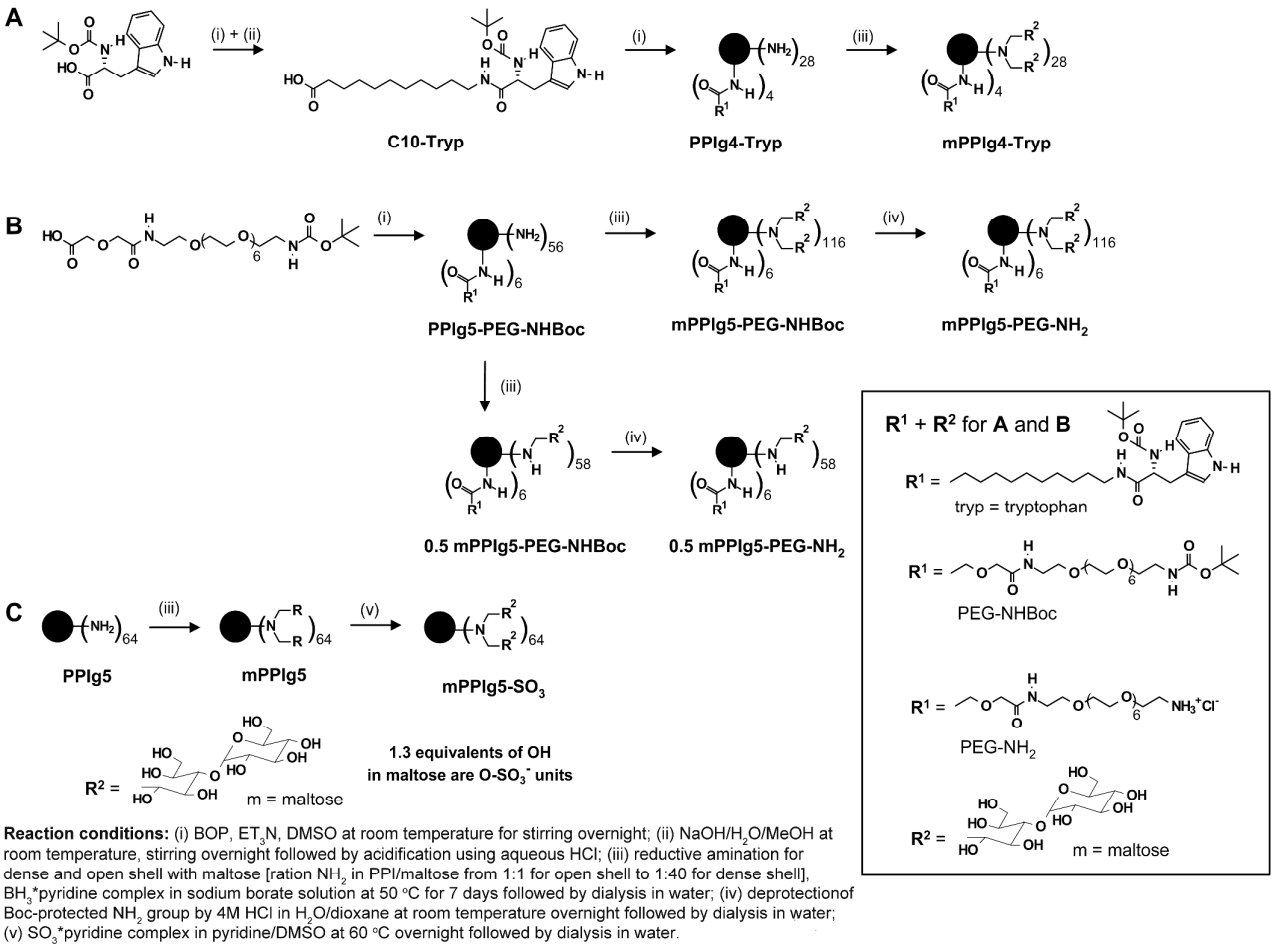

Figure S1. Synthetic pathways of the glycodendrimers used in this study: (A) mPPIg4-Tryp; (B) mPPIg5-PEG-NH_2 and 0.5 mPPIg5-PEG-NH_2; (C) mPPIg5-SO_3.

The synthesis of mPPIg5-PEG-NH_2, 0.5 mPPIg5-PEG-NH_2, mPPIg5-SO_3 and mPPIg4-Tryp is summarized in Figure S1.

The key step in synthesizing mPPIg5-PEG-NH_2 and 0.5 mPPIg5-PEG-NH_2 is the attachment of 6 BOP-activated HO_2C-PEG-NHBoc molecules to the PPIg5 surface. This produces the precursor PPIg5-PEG-NHBoc. Characterization of the structural units of PPIg5-PEG-NHBoc was generally done by ^1H NMR spectroscopy. ^1H NMR spectroscopy can be used to determine the degree of coupled HO_2C-PEG-NHBoc on the PPIg5 scaffold. Values between 5.4 and 5.7 were calculated for the amino spacered entity HO_2C-PEG-NHBoc (Figure S7). From this value, 6 PEG spacered HO_2C-PEG-NHBoc units were assumed for calculating the theoretical Mw (Table S1) of mPPIg5-PEG-NH_2 and 0.5 mPPIg5-PEG-NH_2. MALDI-TOF-MS studies on PPIg5-PEG-NHBoc only revealed decomposition. The true substitution degree of HO_2C-PEG-NHBoc on the PPIg5 scaffold could not be determined. PPIg5-PEG-NHBoc underwent reductive amination to produce mPPIg5-PEG-NHBoc and 0.5 mPPIg5-PEG-NHboc. 0.5 mPPIg5-PEG-NHboc was characterized by ^1H and ^{13}C NMR (Figure S8). The NMR demonstrated that HO_2C-PEG-NHBoc should not be cleaved from the PPIg5 scaffold during the reductive amination process. After reductive amination the Boc-group of protected amino groups is 1.4-1.5 ppm for 0.5 mPPIg5-(PEG-NHBoc) and mPPIg5-(PEG-NHBoc) (Figure S8 for 0.5 mPPIg5-PEG-NHBoc). mPPIg5-(PEG-NHBoc) and 0.5 mPPIg5-(PEG-NHboc) were purified by dialysis and freeze drying before undergoing hydrolysis of the Boc-group to yield the final end-products mPPIg5-PEG-NH_2 and 0.5 mPPIg5-PEG-NH_2. 0.5 mPPIg5-PEG-NH_2 was characterized by ^1H and ^{13}C NMR (Figure S9) and LILBID-MS (Table S1). The dense shell glycodendrimer mPPIg5-PEG-NH_2 was characterized by ^1H NMR and LILBID-MS (Table S1). mPPIg5-PEG-NH_2 and 0.5 mPPIg5-PEG-NH_2 can be viewed as octopus like molecules, consisting of long flexible PEG arms in addition to peripheral cationic amino groups.

mPPIg5-SO_3 is produced by sulfation of the dense shell glycodendrimer mPPIg5 (Figure 1A). mPPIg5 is produced by the reductive amination of PPIg5 in the presence of excess maltose (Figure S1). mPPIg5-SO_3 was characterized by elemental analysis, ^1H NMR and LILBID-MS. The most important aspect in the sulfation process is avoiding the degradation of mPPIg5 maltose units. pH-dependent zeta-potential measurements showed that mPPIg5-SO_3 is in a deprotonated state from pH 3 to pH 10 (Figure 14S). This demonstrates that the sulfation of the mPPIg5 scaffold was successful.

The synthesis of mPPIg4-Tryp requires C10-Tryp. C10-Tryp is produced by a two-step synthetic approach (Figure S1). Boc-protected amino acid tryptophan is converted to a methyl ester of C10-Tryp through the use of 11-aminoundecanoic acid methyl ester hydrochloride. Basic hydrolysis of the methyl ester of C10-Tryp then yields the desired C10-Tryp. The C10-Tryp was characterized by ^{1}H and ^{13}C NMR (Figure S11). Conversion of BOP-activated C10-Trp (4 equivalents) with PPIg4 produces PPIg4-Tryp with ~4 attached C10-Tryp substituents (Figure S12). Reductive amination of PPIg4-Tryp in the presence of excess maltose produces the final end product of the dense shell glycodendrimer mPPIg4-Tryp. mPPIg4-Tryp was characterized by ^{1}H NMR (Figure S13) and LILBID-MS (Table S1).

3 Molecular weight of compounds used in this study

Table S1. Molecular weight (M_w) of PPI glycodendrimers mPPIg5-(PEG-NH_2), 0.5 mPPIg5-(PEG-NH_2), mPPIg4-Tryp and PPIg5-SO_3 based on theoretical calculations for their precursors. M_w determined by LILBID-MS.

	M_w g/mol	**Functional group (spacered)**	**Maltose units**	**M_w g/mol**	**Maltose units**
	Theoretical	***Theoretical***	***Theoretical***	***Observed***	***Observed***
HO_2C-PEG-NHBoc[a]	584.65	-	-	-	-
PPIg5-(PEG-NHBoc)	10,562	6 x PEG-NHBoc	-	-	-
mPPIg5-(PEG-NHBoc)	48,508	6 x PEG-NHBoc	116	45,600	107
mPPIg5-(PEG-NH_2)	48,112	6 x PEG-NH_2	116	40,720	93
0.5 mPPIg5-(PEG-NHBoc)	29,250	6 x PEG-NHBoc	58	27,150	51
0.5 PPIg5-(PEG-NH_2)	29,138	6 x PEG-NH_2	58	25,600	47
C10-Tryp (methyl ester)	503.67	-	-	-	-
C10-Tryp	489.65	-	-	-	-
PPIg4-Tryp	5,389	4 x C10-Tryp	-	-	-
mPPIg4-Tryp	23,708	4 x C10-Tryp	56	23,660	56
mPPIg5	48,933	-	128	46,500	120
PPIg5-SO_3[b]	-	-	-	59,000	120 (with 156 sulfate groups)

[a] Substituent for 0.5 PPIg5-(PEG-NH_2) and PPIg5-(PEG-NH_2); [b] Calculation of the theoretical Mw for PPIg5-SO_3 is not realistic due to the limited reaction of OH groups in maltose units.

4 Synthesis of 0.5 mPPIg5-PEG-NH2

Synthesis of the precursor PPIg5-PEG-NHBoc **(Figure S1)**

α-tert-Butyloxycarbonylamino-ω-diglycolic acid-octa(ethylene glycol) (0.23 g, 0.39 mmol) and BOP (0.17 g, 0.39 mmol) were dissolved in anhydrous DMSO (10 mL) under Ar atmosphere. The reaction solution was stirred for 1 hour at room temperature. A solution of PPIg5 dendrimers (DAB-Am64) (0.44 g, 0.065 mmol) and triethylamine (0.3 mL) in anhydrous DMSO (10 mL) were added and the reaction mixture stirred at room temperature for 24 hours under Ar atmosphere. The crude product was purified by dialysis towards deionised water for 1 day by exchanging deionised water intensively. Precursor PPIg5-PEG-NHBoc was obtained from freeze drying as a white solid (0.64 g, 93%).

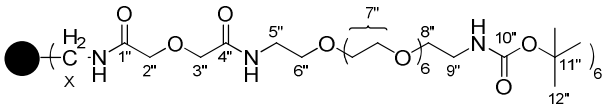

^{1}H NMR (D_2O): 1.42 (12′′), 1.55-1.8 (a, d, g, j, m, p), 2.35-2.7 (b, c, e, f, h, i, k, l, n, o) 2.75-2.9 (q), 3.01 (not assigned), 3.25 (x, 9′′), 3.45 (5′′), 3.57 (8′′), 3.64 (6′′), 3.68 (7′′), 4.11 and 4.12 ppm (2′′, 3′′) (Figure S7-A).

^{13}C NMR (D_2O): 24-29 (a, d, g, j, m, p), 30.7 (12′′), 40.3 (x), 41.4 (q, 5′′), 42.3 (not assigned), 42.6 (9′′), 52-57 (b, c, e, f, h, i, k, l, n, o), 71.6 (6′′), 72.3 (8′′), 72.5 (7′′), 72.8 and 72.9 (2′′ and 3′′), 83.8 (11′′), 161.0 (10′′), 167.4 (not assigned), 174.3 and 174.5 ppm (1′′, 4′′) (Figure S7-B).

Synthesis of the precursor 0.5 mPPIg5-PEG-NHBoc **(Figure S1)**

PPIg5-PEG-NHBoc (0.135 g, 0.01 mmol), maltose (0.39 g, 1.07 mmol, maltose/NH_2 ratio about 1.5) and borane*pyridine complex (0.27 mL, 2.14 mmol, 8M solution) were dissolved in a sodium borate buffer solution (10 ml, 0.1 M). The reaction mixture was stirred at 50 ◦C for 7 days. The crude product was then purified by dialysis towards deionised water for 4 days. Precursor 0.5 mPPIg5-PEG-NHBoc was obtained by freeze drying as a white solid (0.295 g, 87%). 48 maltose units were attached on to the PPIg5 scaffold as determined by the ^{1}H NMR approach described previously.[2] The calculation of the M_w for 0.5 mPPIg5-PEG-NHBoc was based on the final conversion step in the synthesis of 0.5 mPPIg5-PEG-NH_2.

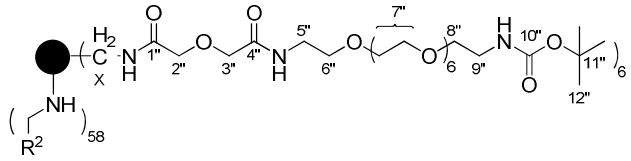

[1]H NMR (D_2O): 1.43 (12′′), 1.5-2.1 (a, d, g, j, m, p), 2.25-3.2 (b, c, e, f, h, i, k, l, n, o, q, 1′), 3.25 (x, 9′′), 3.4-4.5 (2-6, 2′-6′, 2′′, 3′′, 5′′-8′′), 5.05-5.35 ppm (1) (Figure S8-A).

[13]C NMR (D_2O): 23-29 (a, d, g, j, m, p), 30.7 (12′′), 40.2 (x), 41.4 (5′′), 42.6 (9′′), 48-51 (q, mono-maltosylated), 52-57 (b, c, e, f, h, i, k, l, n, o, q, 1′), 63-67 (6, 6′), 69.8 (2′), 71-79 (2-5, 3′, 5′, 2′′, 3′′), 72.4 (7′′), 83-86 (4′, 11′′), 99.4 and 103.4 (1), 160.7 (10′′), 174.1 ppm (1′′, 4′′) (Figure S8-B).

LILBID-MS (Tris/HCl; pH 7.5): *m/z* calcd: 29250; found: 27150 [M^{-1}].

Synthesis of 0.5 mPPIg5-PEG-NH$_2$ **(Figure S1)**

0.5 mPPIg5-PEG-NHBoc (0.151 g, 0.005 mmol) was dissolved in 10 mL water and 20 ml HCl (4M in dioxane) added. The reaction mixture was stirred overnight at room temperature. The crude product was purified by dialysis towards deionised water for 6 hours. 0.5 mPPIg5-PEG-NH_2 was obtained (0.138 g, 95%) by freeze drying as a white solid. The M_w of 0.5 mPPIg5-PEG-NH_2 was determined by LILBID-MS (see below and Table S1).

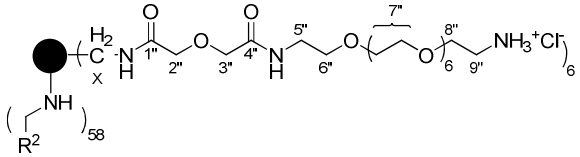

[1]H NMR (D_2O): 1.6-2.0 (a, d, g, j, m, p), 2.45-3.15 (b, c, e, f, h, i, k, l, n, o, q, 1′), 3.20 (9′′), 3.29 (x), 3.3-4.2 (2-6, 2′-6′, 2′′, 3′′, 5′′-8′′), 5.12 ppm (1) (Figure S9-A).

[13]C NMR (D_2O): 23-28 (a, d, g, j, m, p), 40.0 (x), 41.4 (5′′), 42.0 (9′′), 48-50 (q, mono-maltosylated), 52-56 (b, c, e, f, h, i, k, l, n, o, q, 1′), 63.3 (6), 65.2 and 65.7 (6′), 69.0-77 (2-5, 2′, 3′, 5′, 2′′, 3′′, 6′′- 8′′), 84.5 (4’), 103.4 (1), 163.6 and 167.0 (not assigned), 174-176 ppm (1′′, 4′′) (Figure S9-B).

LILBID-MS (Tris/HCl; pH 7.5): *m/z* calcd: 29138; found: 25600 [M^{-1}].

5 Synthesis of mPPIg5-PEG-NH_2

The synthesis of the precursor **PPIg5-PEG-NHBoc** (**Figure S1**) is described above.

Synthesis of the precursor mPPIg5-PEG-NHBoc (**Figure S1**)

Precursor PPIg5-PEG-NHBoc (0.528 g, 0.05 mmol), maltose (32.88 g, 91 mmol) and borane*pyridine complex (22.80 mL, 180 mmol, 8M solution) were dissolved in a sodium borate buffer solution (50 ml, 0.1 M). The reaction mixture was stirred at 50 ◦C for 7 days. The crude product was purified by dialysis towards deionised water for 4 days. The dense shell glycodendrimer mPPIg5-PEG-NHBoc was obtained by freeze drying as a white solid (1.84 g, 76%).

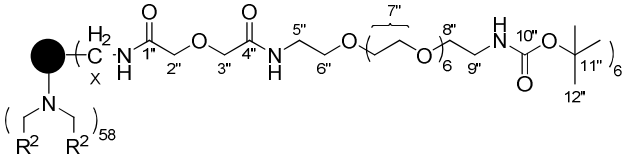

^{1}H NMR (D_2O): 1.44 (12´´), 1.5-2.1 (a, d, g, j, m, p), 2.4-3.4 (b, c, e, f, h, i, k, l, n, o, q, x, 1´, 9´´), 3.4-4.4 (2-6, 2´-6´, 5´´-8´´), 5.0-5.3 ppm (1).

LILBID-MS (Tris/HCl; pH 7.5): *m/z* calcd: 48508; found: 45600 [M^{-1}].

Synthesis of mPPIg5-PEG-NH_2 (**Figure S1**)

mPPIg5-PEG-NHBoc (0.291 g, 0.006 mmol) was dissolved in 7 mL water and 14 ml HCl (4M in Dioxane) added. The reaction mixture was stirred overnight at room temperature. The crude product was purified by dialysis towards deionised water for 6 hours. Deprotected dense shell glycodendrimer mPPIg5-PEG-NH_2 was obtained as a white solid by freeze drying (0.22 g, 76%).

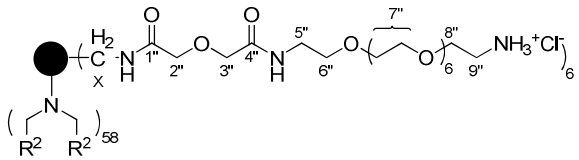

^{1}H NMR (D_2O): ^{1}H NMR: 1.65-2.2 (a, d, g, j, m, p), 2.5-3.3 (b, c, e, f, h, i, k, l, n, o, q, x, 1´, 9´´), 3.4-4.3 (2-6, 2´-6´, 2´´, 3´´, 5´´-8´´), 5.16 ppm (1).

LILBID-MS (Tris/HCl, pH 7.5): *m/z* calcd: 48112; found: 40720 [M^{-1}].

6 Synthesis of mPPIg5-SO_3

Synthesis of the glycodendrimer mPPIg5 (Figure 1 presented in the paper) was described previously.[2]

A suspension of mPPIg5 (0.325 g, 0.007 mmol) in anhydrous DMSO (20 mL) was heated at 100°C for 1h to dissolve mPPIg5. The solution was cooled down to room temperature. Pyridine (1.5 mL, 0.12 mmol) and sulfur trioxide*pyridine complex (1.00 g, 6.32 mmol) were added and the reaction solution stirred overnight at 60°C. The pH was adjusted to neutrality with a 1M NaOH solution. The crude product was purified by dialysis towards deionised water for 4 days by exchanging the deionised water intensively. mPPIg5-SO_3 was obtained as a white solid (0.81 g) by freeze drying.

^{1}H NMR (D_2O): 1.6-2.4 (a, d, g, j, m, p), 2.4-3.4 (b, c, e, f, h, i, k, l, n, o, q, 1´), 3.4-4.7 (2-6, 2´-6´), 4.9-5.5 ppm (1). Significant low field shift of signals of the maltose units compared to the starting material indicates formation of sulfated maltose moieties.

LILBID-MS (Tris/HCl, pH 7.5): found: 59100 [M^{-1}]; calculation of theoretical M_w is not realistic due to limited reaction of OH groups in maltose units.

7 Synthesis of mPPIg4-Tryp

Synthesis of C10-Tryp **(Figure S1)**

Methyl 11-Aminoundecanoate ester hydrochloride (0.400 g, 1.59 mmol, M_w 251.79 g/mol) was dissolved in 20 mL of anhydrous DMF under Ar atmosphere. *Nα*-tert-Butyloxycarbonylamino-*L*-tryptophan (0.484 g, 1.59 mmol, M_w 304.34 g/mol), triethylamine (5.3 mL) and BOP (0.736 g, 1.66 mmol, M_w 442.27 g/mol) were added. The reaction solution was stirred for 24 hour at room temperature under light protection. After evaporation of DMF under vacuum the residual was dissolved in ethyl acetate (100 ml) and washed with water (1x100 mL) and aqueous NaCl solution (2x30 mL). Column chromatography (ethyl acetate/n-heaxane 2:3) with silica gel was used to purify methyl ester of C10-Tryp (0.78 g; 98% yield).

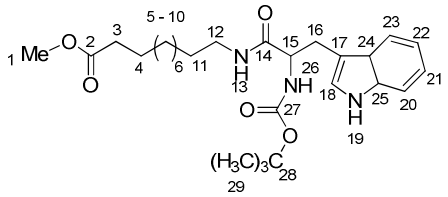

^{1}H NMR (DMSO-d_6): 1.1-1.3 (5-10), 1.32 (29), 1.34 (11), 1.50 (4), 2.27 (3), 2,89 and 3.03 (16), 3.03 (12), 3.57 (1), 4.07 and 4.15 (15, two rotamers of Boc), 6.16 and 6.65 (26, two rotamers of Boc), 6.96 (22), 7.05 (21), 7.10 (18), 7.31 (20), 7.56 (23), 7.75 and 7.80 (13, two rotamers of Boc), 10.76 ppm (19) (Figure S10).

Methyl ester of C10-Tryp (0.300 g, 0.598 mmol, M_w501.66 g/mol) and sodium hydroxide (0.072 g, 1.794 mmol) were dissolved in water (5 mL) and methanol (15 mL). The reaction solution was stirred overnight at room temperature followed by the distillation of water and methanol under vacuum. The solid was dissolved in ice-cold water (2 mL) and acidified with diluted HCl to calibrate the solution to pH 2. The precipitate was isolated by filtration and the light brownish solid dried in a vacuum oven at 40 °C. C10-Tryp (M_w 431.53 g/mol) was yielded at 83% purity (192 mg).

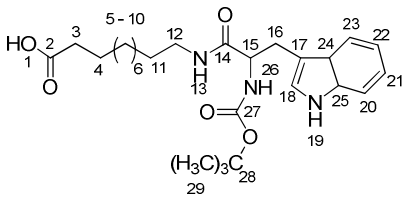

^{1}H NMR (DMSO-d_6): 1.1-1.3 (5-10), 1.32 (29), 1.34 (11), 1.48 (4), 2.18 (3), 2,89 and 3.03 (16), 3.03 (12), 4.07 and 4.15 (15, two rotamers of Boc), 6.17 and 6.65 (26, two rotamers of Boc), 6.96 (22), 7.05 (21), 7.10 (18), 7.32 (20), 7.56 (23), 7.75 and 7.81 (13, two rotamers of Boc), 10.77 (19), 11.9 ppm (1) (Figure S11-A).

^{13}C NMR (DMSO-d_6): 25.40 (4), 27-30.5 (5-11, 16, 29), 34.58 (3), 39.40 (12), 56.08 and 57.2 (15, two rotamers of Boc), 78.79 and 78.9 (28, two rotamers of Boc), 111.13 (17), 112.10 (20), 118.98 (22), 119.34 (23), 121.65 (21), 124.40 (18), 128.28 (24), 136.94 (25), 155.35 and 155.97 (27, two rotamers of Boc), 172.55 (14), 175.36 ppm (2) (Figure S11-B)..

Synthesis of the precursor PPIg4-Tryp (**Figure S1**)

C10-Tryp (0.112 g, 0.23 mmol) was dissolved in anhydrous DMSO (10 mL) under Ar atmosphere and BOP (0.101 g, 0.23 mmol) was added. The reaction solution was stirred at room temperature for 1 hour. A solution of 4th generation PPI dendrimer (DAB-Am32) (0.2 g, 0.06 mmol) and triethylamine (0.3 mL) in anhydrous DMSO (10 mL), prepared under Ar atmosphere, was added and the reaction mixture stirred at room temperature for 24 hours under Ar atmosphere. The crude product was purified by dialysis towards deionised water for 1 day by exchanging deionised water intensively. The precursor PPIg4-Tryp was obtained as a white solid by freeze drying (0.22 g, 68%).

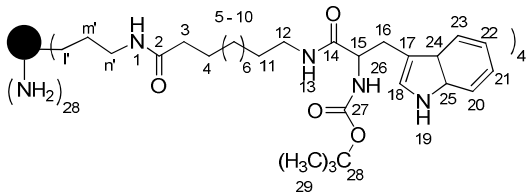

^{1}H NMR (DMSO-d_6): 1.1-1.3 (5-10), 1.31 (29), 1.3-1.7 (a, d, g, j, m, m′, 4, 11), 2.03 (3), 2.1-2.8 (b, c, e, f, h, i, k, l, l′), 2.85-3.1 (12, 16, n'), 4.07 and 4.15 (15, two rotamers of Boc), 6.19 and 6.65 (26, two rotamers of Boc), 6.95 (22), 7.03 (21), 7.09 (18), 7.31 (20), 7.55 (23), 7.79 (13), 7.84 (1), 10.79 ppm (19) (Figure S12-A).

^{13}C NMR (DMSO-d_6): 24-25 (a, d, g, j, m), 25.4 (4), 27-30.5 (5-11, 16, 29, m′), 35.6 (3), 37.0 (n′) (12), 38.6 (12), 51-53 (b, c, e, f, h, i, k, l′), 55.2 (15), 77.9 (28), 110.2 (17), 111.2 (20), 118.1 (22), 118.4 (23), 120.8 (21), 123.5 (18), 127.4 (24), 136.1 (25), 155.1 (27), 171.7 (14), 172.1 ppm (2) (Figure S12-B).

Synthesis of the mPPIg4-Tryp (**Figure S1**)

PPIg4-Tryp (0.16 g, 0.03 mmol), maltose (13.1 g, 360 mmol) and borane*pyridine complex (9 mL, 72 mmol, 8M solution) were dissolved in a sodium borate buffer solution (50 mL, 0.1 M). The reaction mixture was stirred at 50 ◦C for 7 days. The crude product was purified by dialysis towards deionised water for 4 days. mPPIg4-Tryp was obtained as a white solid by freeze drying (0.58 g, 81%).

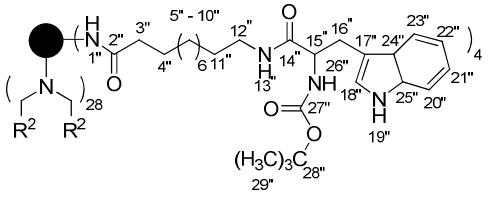

^{1}H NMR (D_2O): 0.9-1.5 (4´´-11´´), 1.41 (29''), 1.5-2.1 (a, d, g, j, m), 2.23 (2´´), 2.3-3.3 (b, c, e, f, h, i, k, l, n, 1´, 12´´, 16´´), 3.4-4.4 (2-6, 2´-6´, 15´´), 5.0-5.3 (1), 6.8-7.8 ppm (18´´, 20´´-23´´) (Figure 13-SI).

LILBID-MS (Tris/HCl, pH 7.5): *m/z* calcd: 23708; found: 23660 [M^{-1}].

8 NMR spectra of mPPIg4 and mPPIg5

The ^{1}H and ^{13}C NMR spectra of 0.5 mPPIg5-PEG-NH_2, mPPIg5-PEG-NH_2, mPPIg5-SO_3 and mPPIg4-Tryp is presented later. To help aid the understanding of this data, the ^{1}H and ^{13}C NMR spectra of mPPIg4 and mPPIg5 is included here. The data includes (A) the signal assignment for maltose units on the PPI scaffold and (B) signal assignment for the PPIg4 and PPIg5 scaffold.

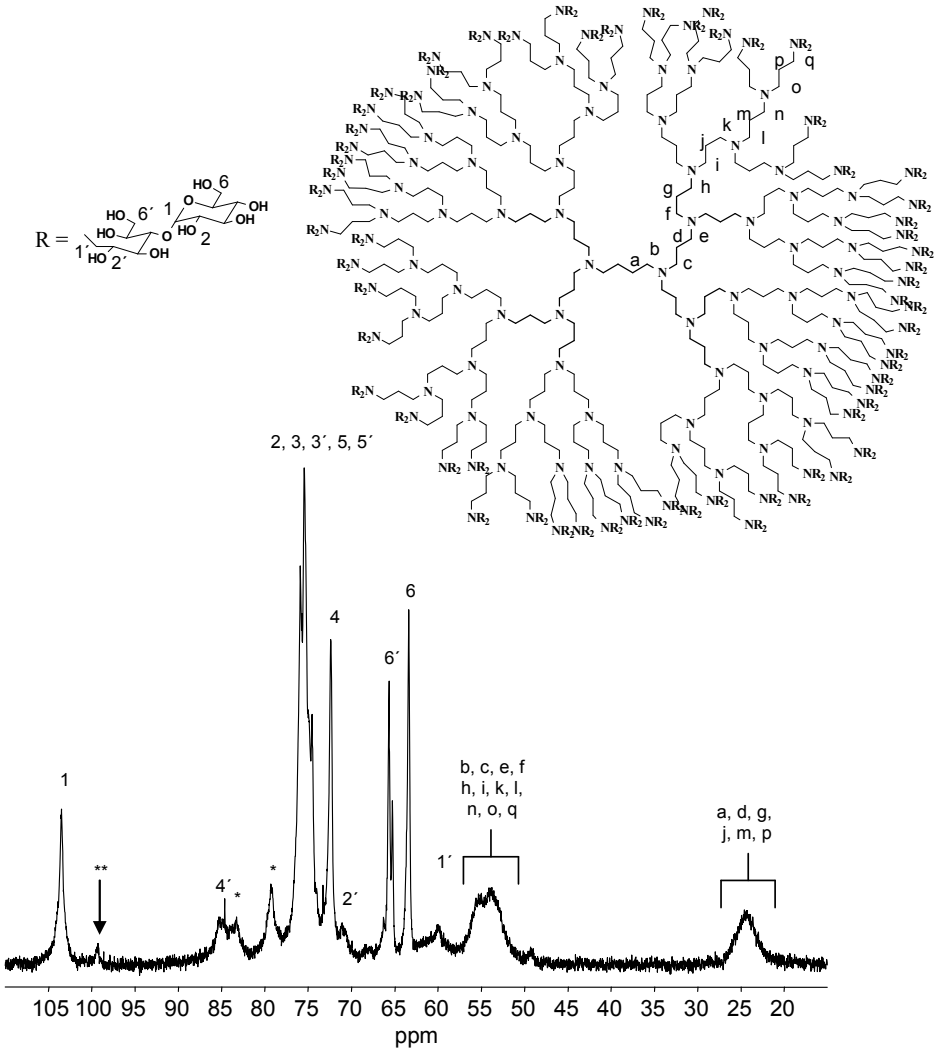

Figure S2. ^{13}C NMR spectrum of mPPIg5 in D_2O (* indicates non-assigned signals). **Anomeric C atom of the maltose. From Klajnert et al,: The influence of densely organized maltose shells on the biological properties of poly(propylene imine) dendrimers: new effects dependent on hydrogen bonding. Chem. Eur. J, 2008, 14, 7030. Copyright Wiley-VCH Verlag GmbH & Co. KGaA. Reproduced with permission.

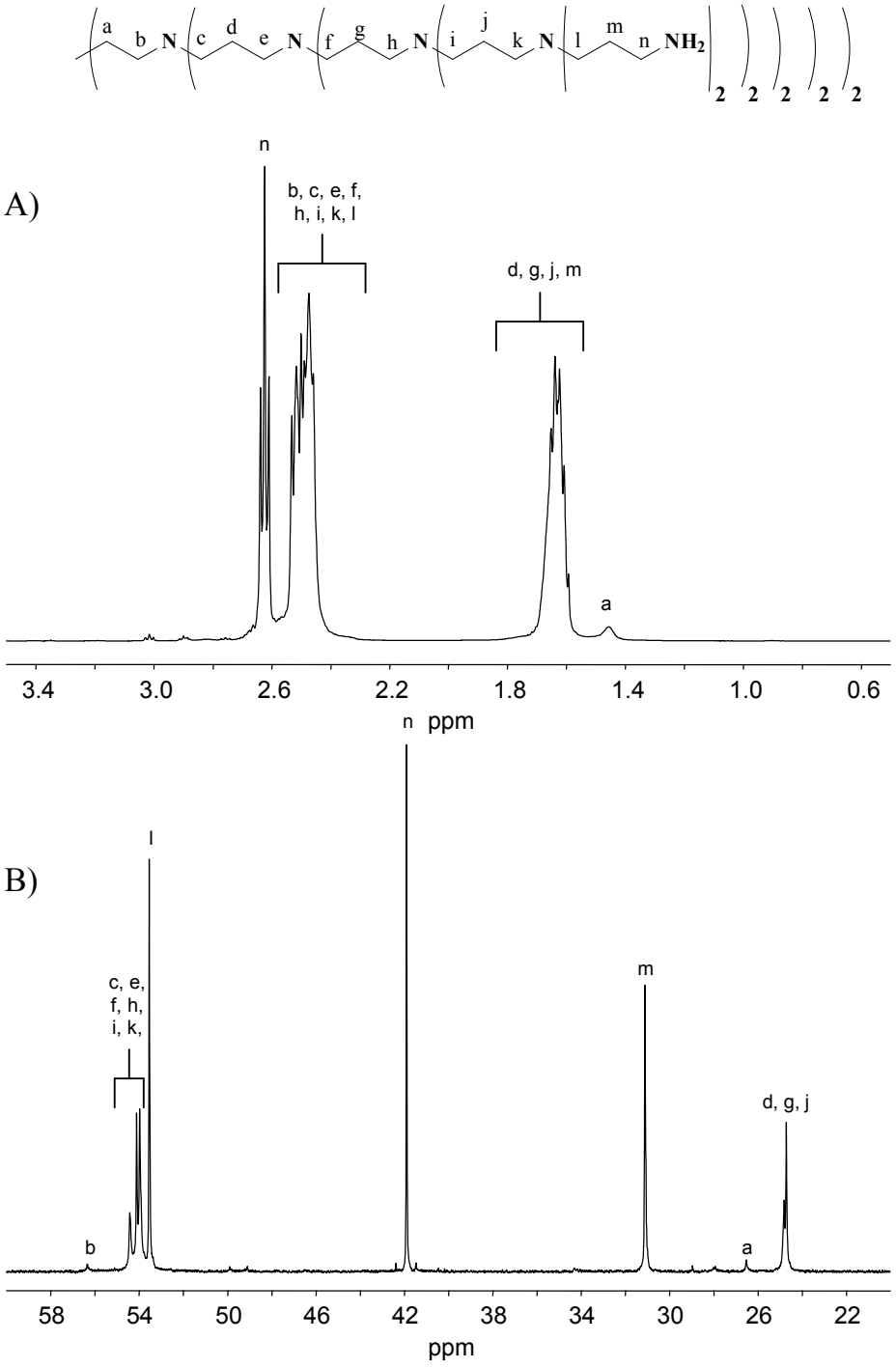

Figure S3. (A) ^{1}H and (B) ^{13}C NMR spectrum of PPIg4 in D_2O.

From Klajnert et al,: The influence of densely organized maltose shells on the biological properties of poly(propylene imine) dendrimers: new effects dependent on hydrogen bonding. Chem. Eur. J, 2008, 14, 7030. Copyright Wiley-VCH Verlag GmbH & Co. KGaA. Reproduced with permission.

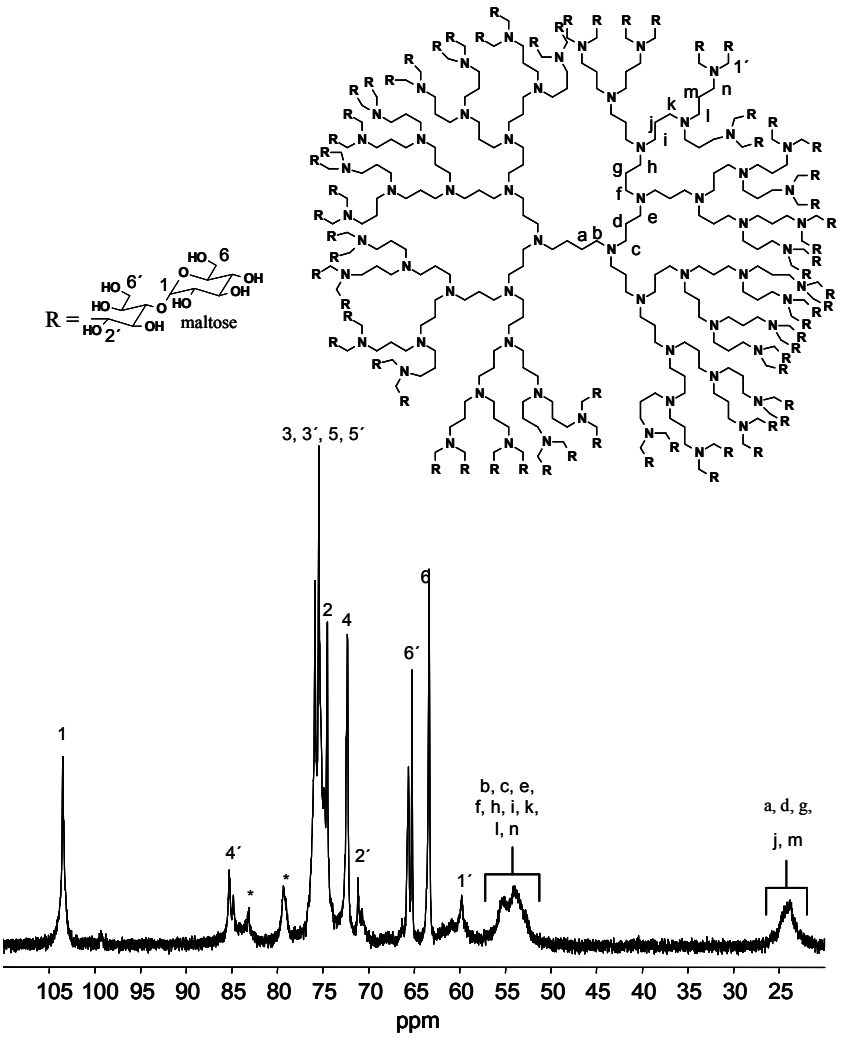

Figure S4. ^{13}C NMR spectrum of mPPIg4 in D_2O. *Non-assigned maltose signals.

From Klajnert et al,: The influence of densely organized maltose shells on the biological properties of poly(propylene imine) dendrimers: new effects dependent on hydrogen bonding. Chem. Eur. J, 2008, 14, 7030. Copyright Wiley-VCH Verlag GmbH & Co. KGaA. Reproduced with permission.

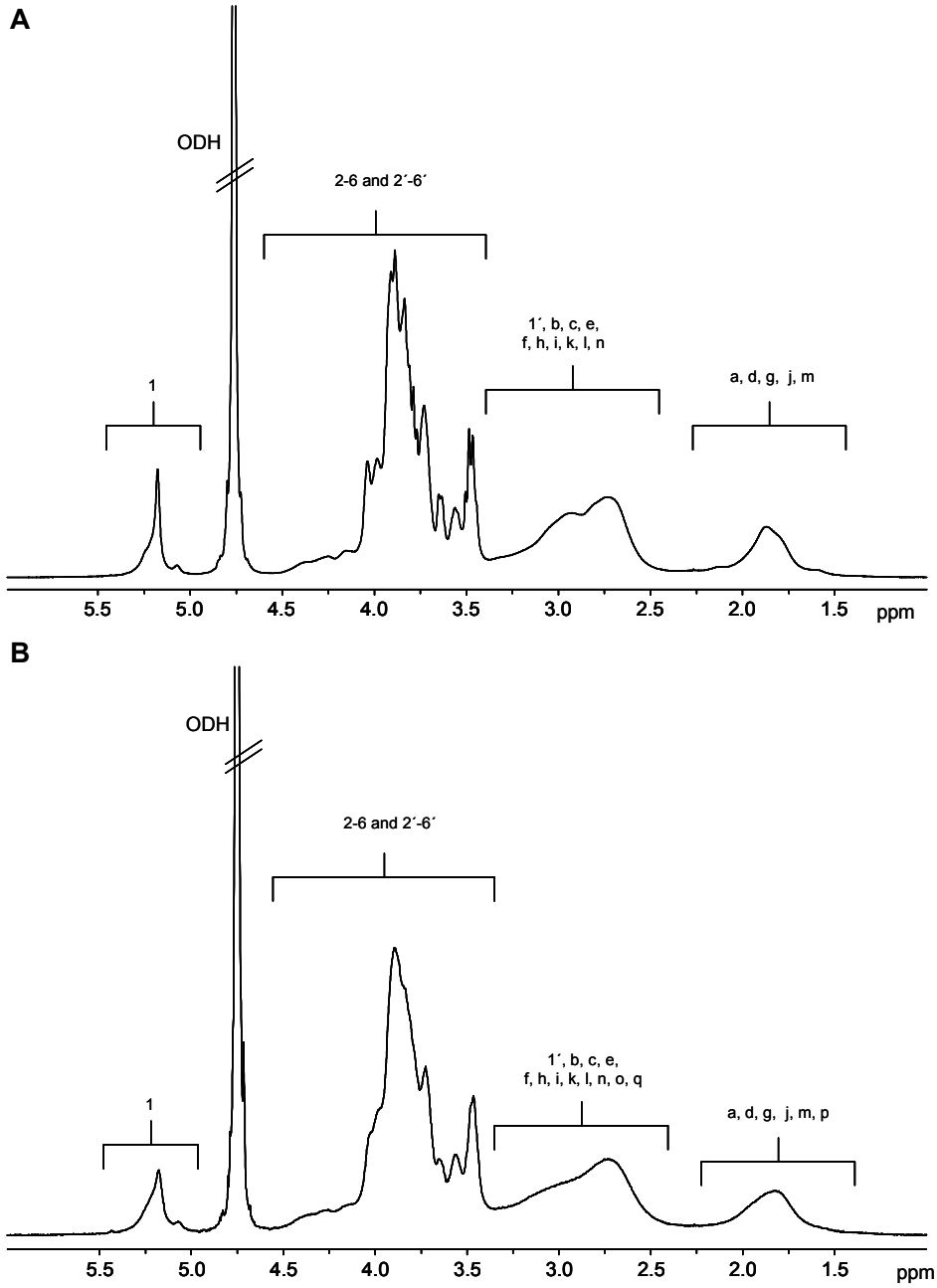

Figure S5. ^{1}H NMR spectra of (A) mPPIg4 and (B) mPPIg5 in D_2O. mPPIg5 data (B) from Klajnert et al,: The influence of densely organized maltose shells on the biological properties of poly(propylene imine) dendrimers: new effects dependent on hydrogen bonding. Chem. Eur. J, 2008, 14, 7030. Copyright Wiley-VCH Verlag GmbH & Co. KGaA. Reproduced with permission.

9 ^{1}H NMR spectra of HO_2C-PEG-NHBoc

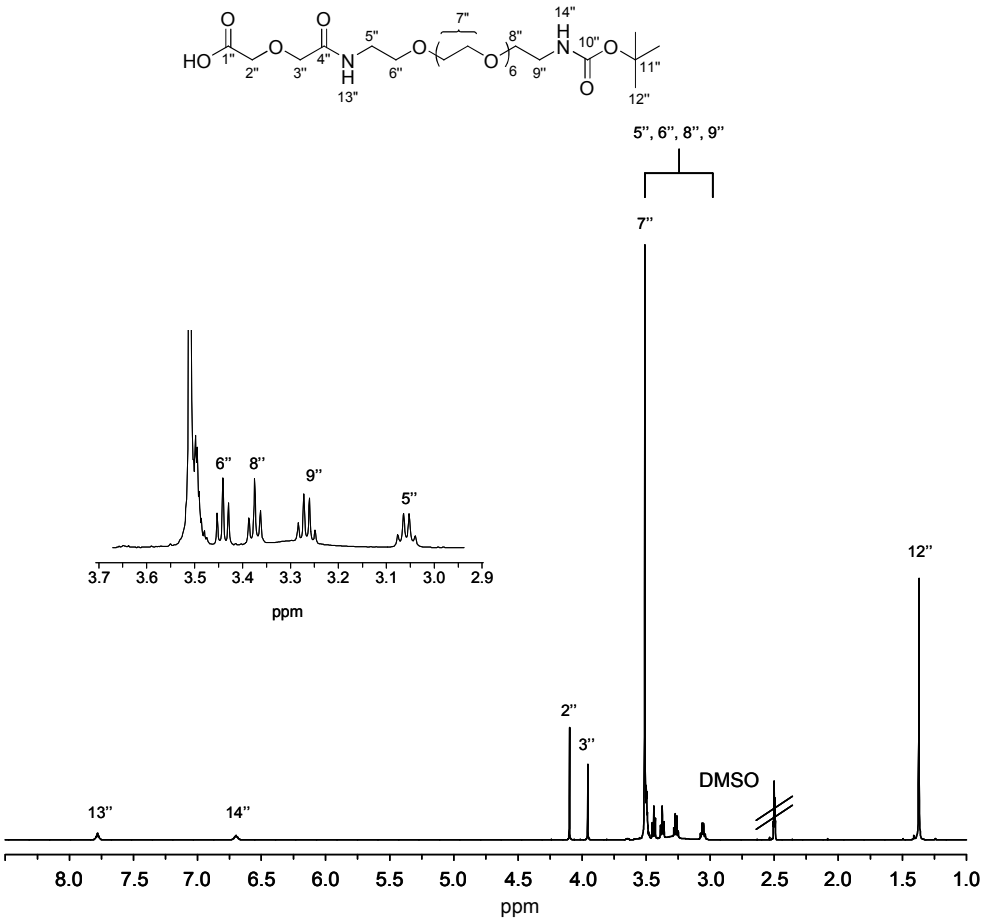

Figure S6. ^{1}H NMR of HO_2C-PEG-NHBoc in DMSO-d6. This molecule was used as a precursor for synthesizing PPI glycodendrimers mPPIg5-PEG-NH_2 and 0.5 mPPIg5-PEG-NH_2.

10 NMR spectra of PPIg5-PEG-NHBoc and degree of substitution of PEG unit (HO_2C-PEG-NHBoc) on PPIg5 surface

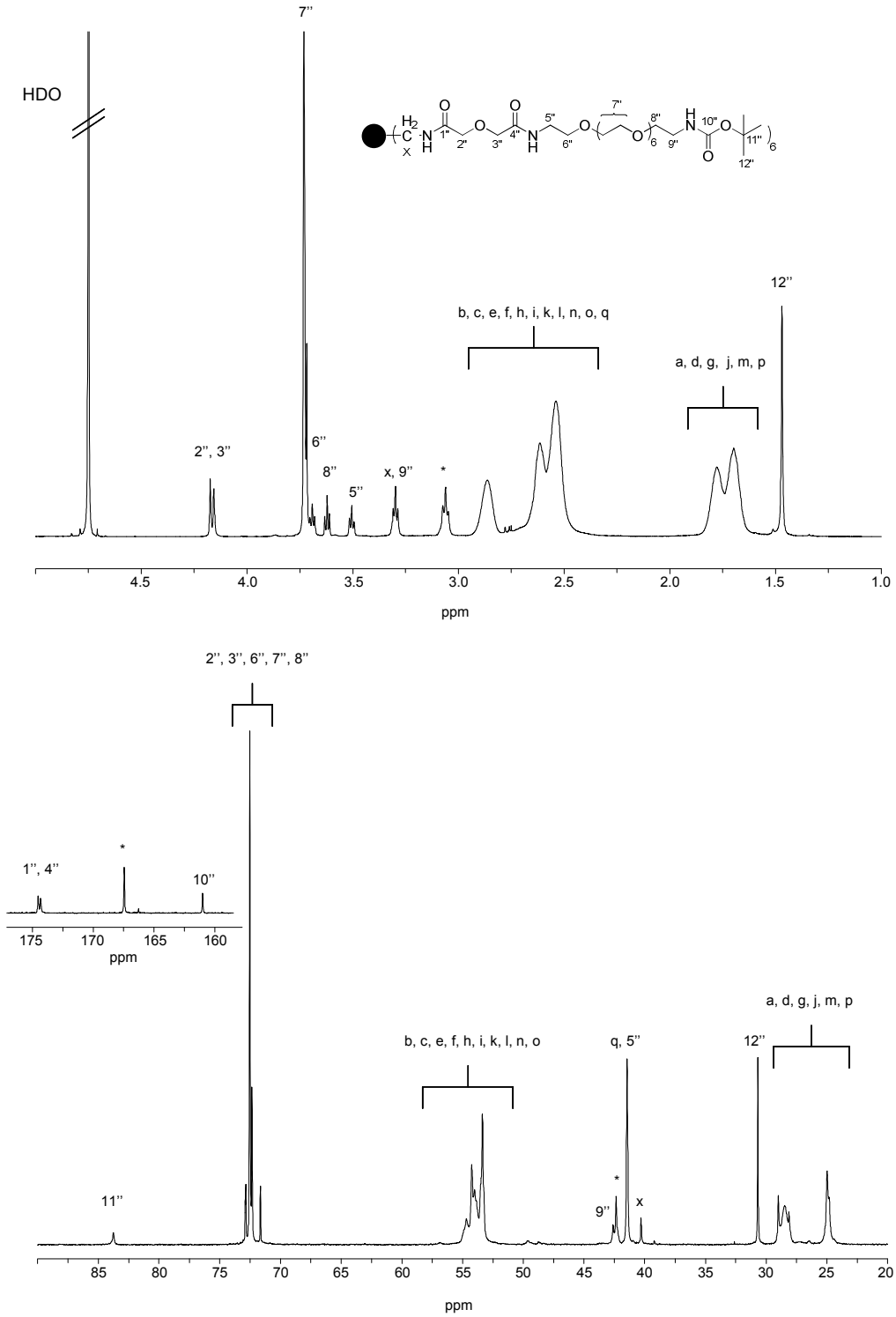

Figure S7. ^{1}H and ^{13}C NMR of PPIg5-PEG-NHBoc in D_2O. This molecule was used as a precursor for synthesizing PPI glycodendrimers mPPIg5-PEG-NH_2 and 0.5 mPPIg5-PEG-NH_2. Assignment of a-q for 5^{th} generation PPI scaffold is presented in Figure S2.

The ^{1}H NMR spectrum of PPIg5-PEG-NHBoc can be used to determine the level of coupled PEG units (HO_2C-PEG-NHBoc) on the surface of the PPIg5 scaffold: The integral value of the four protons of 2′′ and 3′′ (~ 4.2 ppm) gives the intensity of one proton of the attached PEG units. The integral value of the 1.25 – 2.0 ppm region gives the intensity of protons a, d, g, j, m, p of the PPIg5 scaffold and 12′′. This large region was used to avoid integration errors due to signal overlap. This integral value is corrected by the integral of 12′′ calculated from the intensity of 2′′ and 3′′. The corrected integral represents 252 protons of PPIg5 and thus the intensity of one proton of the PPIg5 can be calculated. PPIg5 contains 64 amino endgroups. Relating the intensity of 64 amino protons of PPIg5 to the intensity of the PEG unit gives the degree of modification. This method was used to calculate 5.6 PEG units per PPIg5 macromolecule. Thus, 6 PEG units per PPIg5 macromolecule were assumed for calculating the theoretical M_w of the glycodendrimers mPPIg5-PEG-NH_2 and 0.5 mPPIg5-PEG-NH_2 (Table S1).

11 NMR spectra of 0.5 mPPIg5-PEG-NHBoc

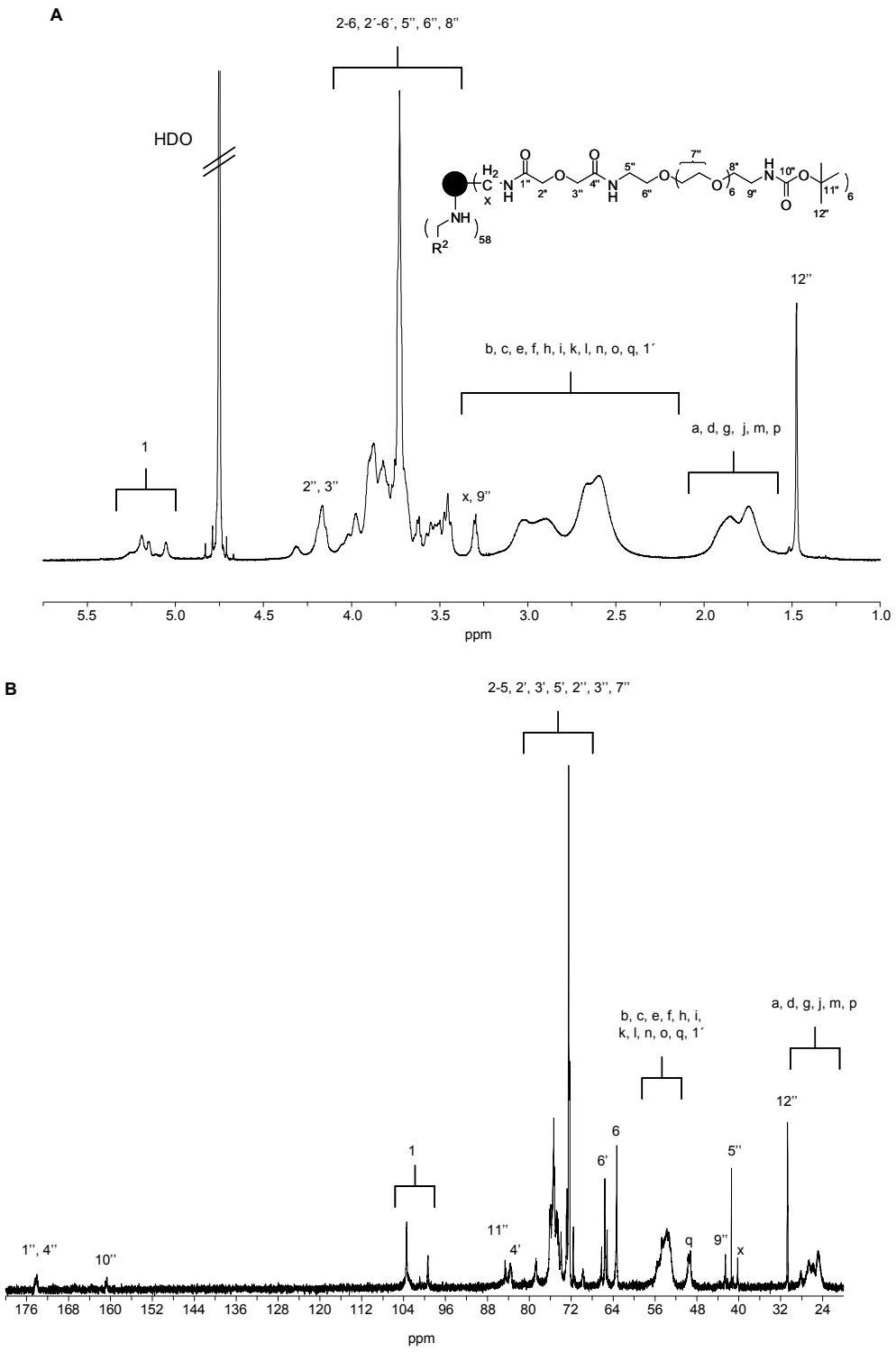

Figure S8. (A) ^{1}H and (B) ^{13}C NMR spectrum of 0.5 mPPIg5-PEG-NHBoc in D_2O. * non-assignable ^{13}C NMR signal. Assignment of 1-6 and 1´-6´ (maltose unit as R^2) is presented in Figure S1. Assignment of a-q for the 5th generation PPI scaffold is presented in Figure S2.

12 NMR spectra of 0.5 mPPIg5-PEG-NH_2

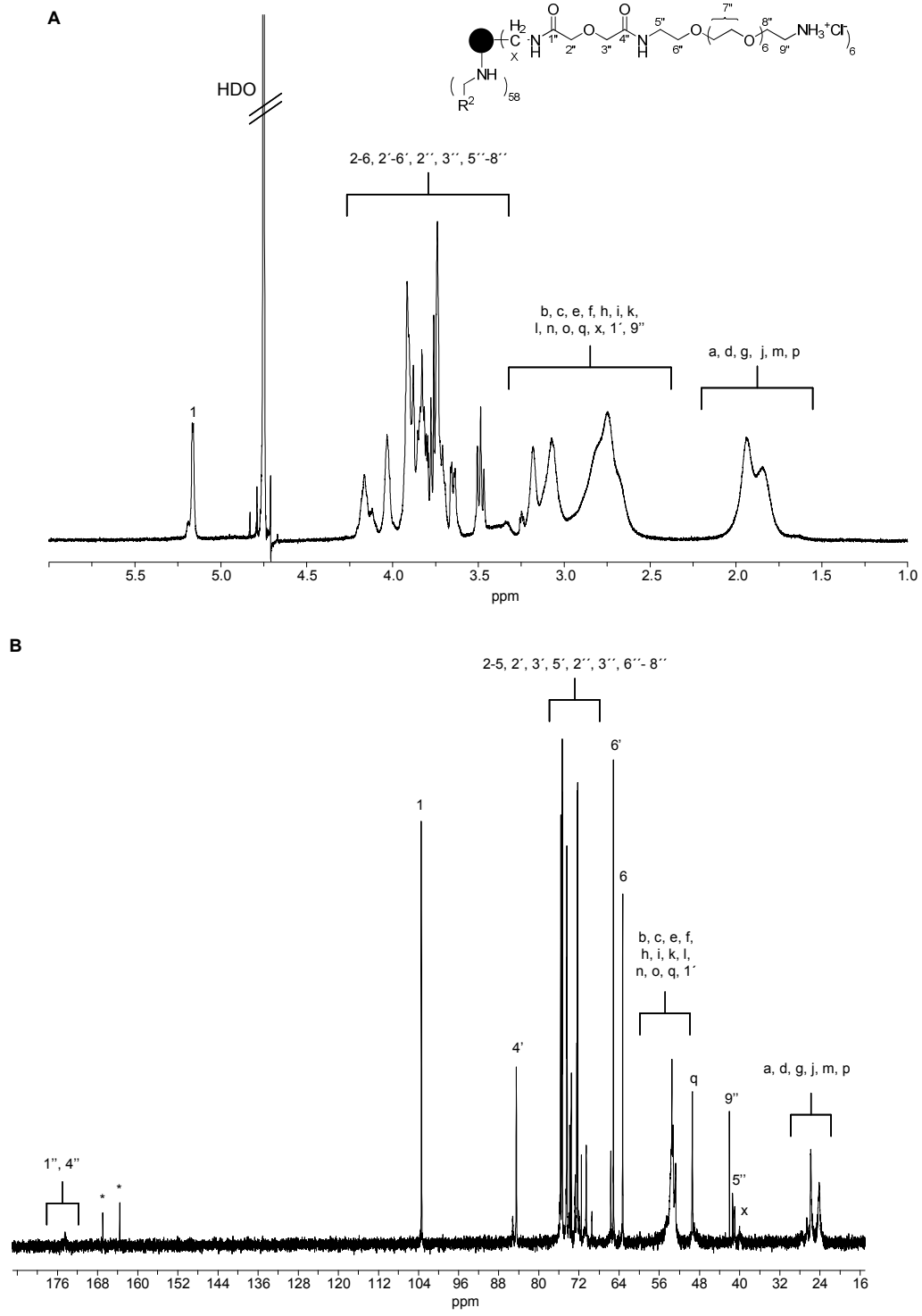

Figure S9. (A) ^{1}H and (B) ^{13}C NMR spectrum of 0.5 mPPIg5-PEG-NH_2 in D_2O. * non-assignable ^{13}C NMR signal. Assignment for 1-6, 1´-6´ (maltose unit as R^2) and a-q for 5th generation PPI scaffold is presented in Figure S2.

13 NMR spectra of methyl ester of C10-Tryp, C10-Tryp-COOH, PPIg4-Tryp and mPPIg4-Tryp

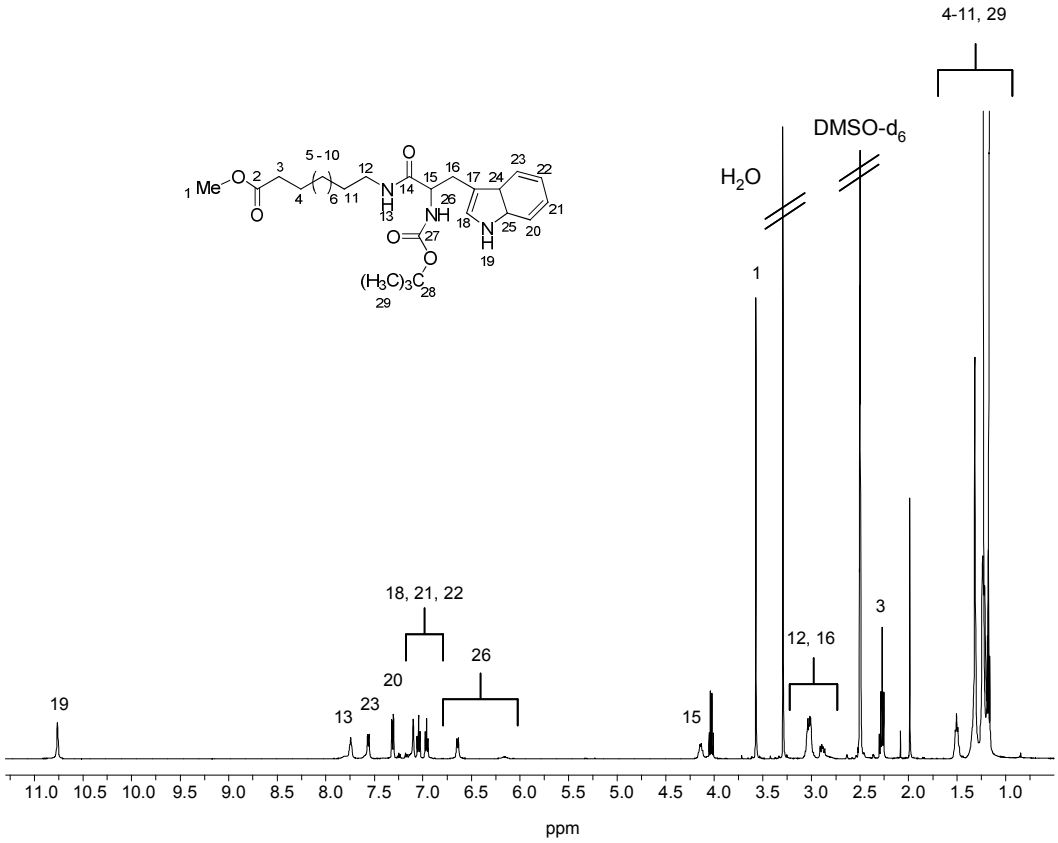

Figure S10. ^{1}H NMR spectrum of methyl ester of C10-Tryp in DMSO-d6.

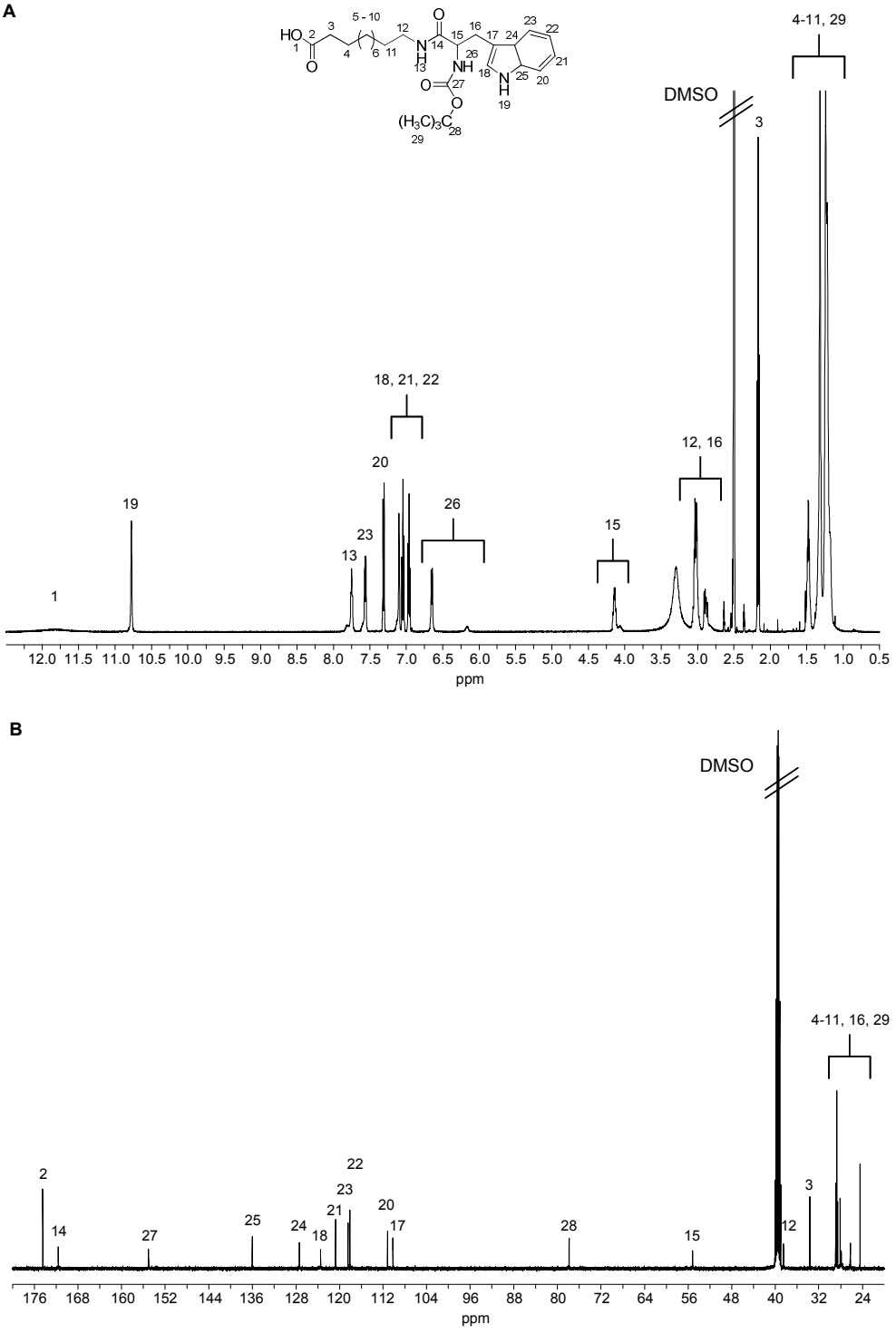

Figure S11. (A) ^{1}H and (B) ^{13}C NMR spectrum of C10-Tryp-COOH in DMSO-d6.

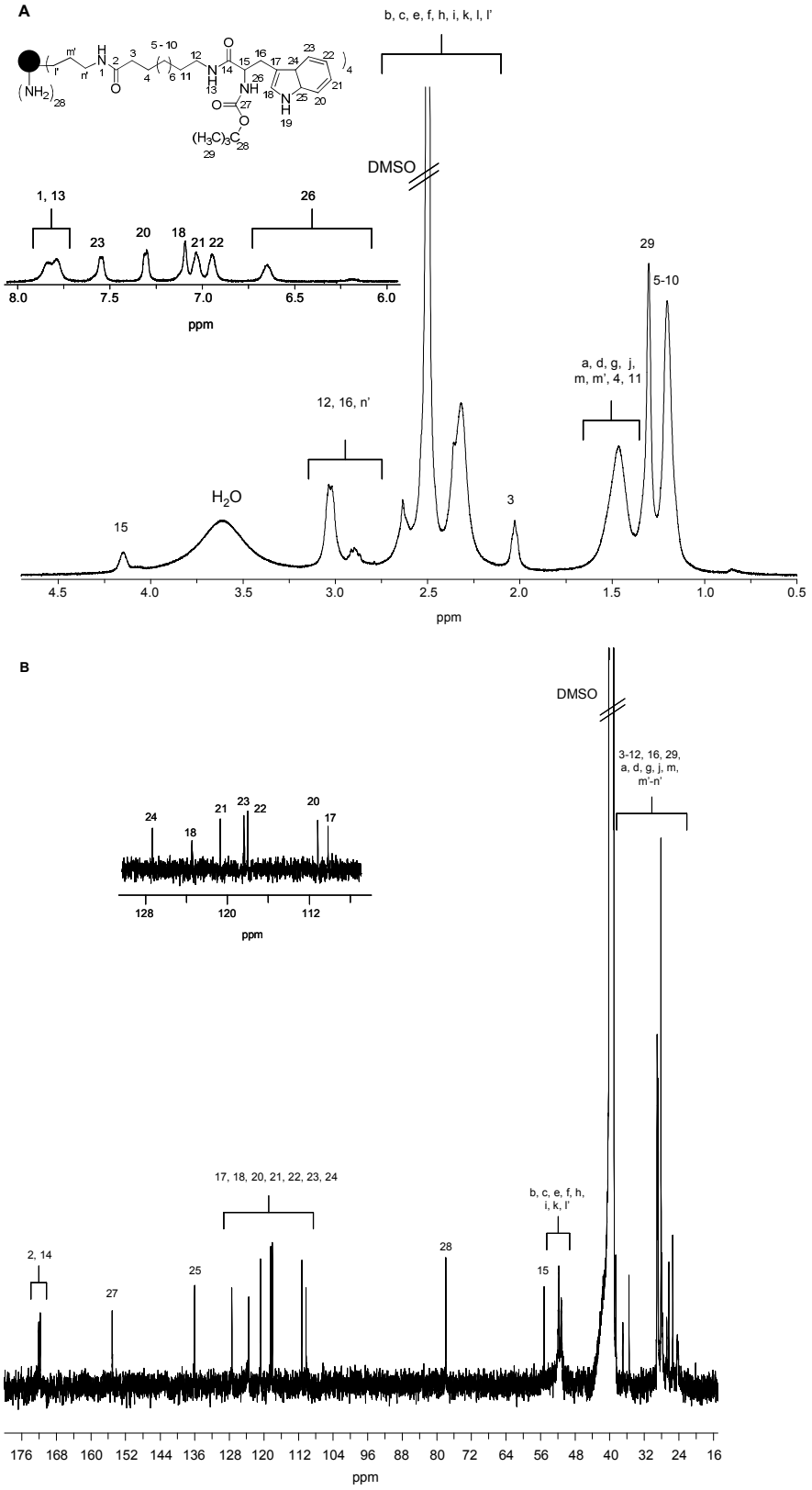

Figure S12. (A) ^{1}H and (B) ^{13}C NMR spectrum of PPIg4-Tryp in DMSO-d6. Assignment of a-n for the 4th generation PPI scaffold is presented in Figure S3.

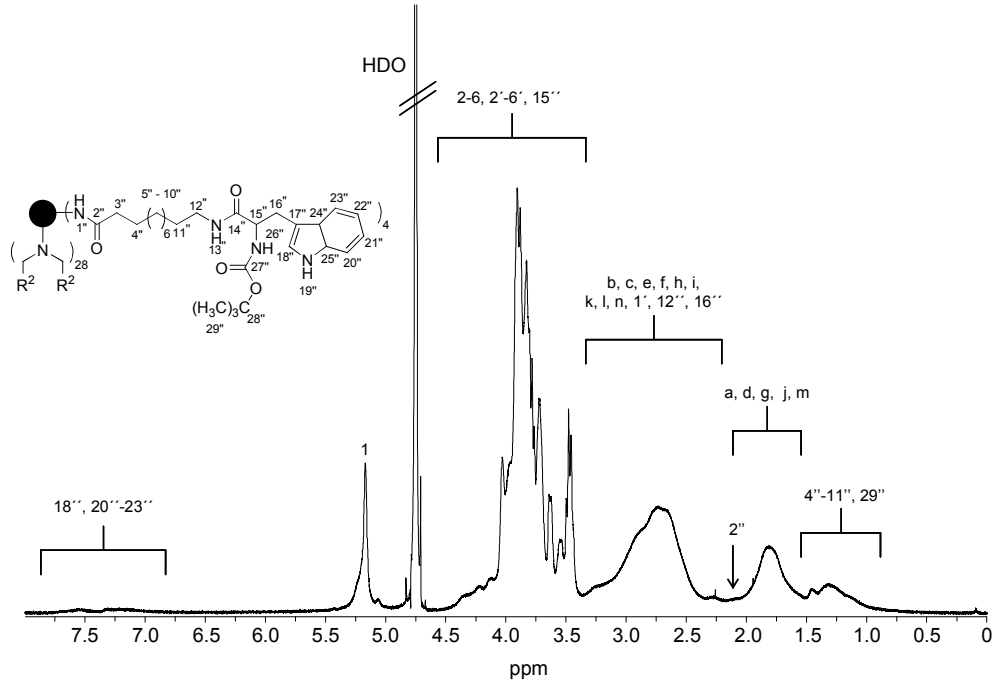

Figure S13. (A) ^{1}H NMR spectrum of mPPIg4-Tryp in D_2O. Assignment for 1-6 and 1´-6´ (maltose unit = R^2) is presented in Figure S4. Assignment of a-n for the 4th generation PPI scaffold is presented in Figure S3.

14 pH-dependent zeta potential measurement

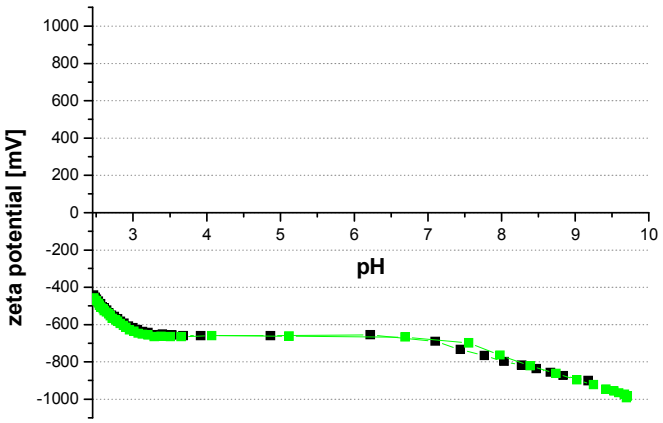

Figure S14. pH-dependent zeta-potential of mPPIg5-SO_3 possessing no isoelectronic point. Over the measured pH range, the macromolecule is deprotonated and anionic due to the presence of strong acid substituents in maltose shell of mPPIg5-SO_3.

15 Molecular modeling of the mPPIg5 dendrimer

Methods.

The 3D model of dendrimer structure was created using Materials Studio software package from Accelrys Inc. The individual dendrimer residues were parametrized using Antechamber, the module of Amber 12 package.[3] The AM1-BCC approach[4] was used for calculation of partial charges. The GAFF (Generalized Amber Force Field) and GLYCAM06 force fields were chosen for parametrization of maltose-modified PPI dendrimer.[5,6] Dendrimer was solvated in explicit water (TIP3P model). This molecular system was subsequently minimized (5000 steps with 2 kcal/(mol Å2) restraint + 5000 without restraint), heated (200 ps of Molecular dynamics in NVT ensemble) to 310K and then simulated using Molecular dynamics in NPT ensemble for 34 ns. Hydrogens were constrained with the SHAKE algorithm[7] to allow 2 fs time step. Langevin thermostat with collision frequency 2 ps was used for all molecular dynamics runs.[8] The pressure relaxation time for weak-coupling barostat was 2 ps. Particle mesh Ewald method (PME)[9] was used to treat long range electrostatic interactions under periodic conditions with a direct space cutoff of 10 angstroms. The same cutoff was used for van der Waals interactions. The pmemd.cuda module from Amber12 was used for all the above described simulation steps. For the structural analyses (Rg, RDF) the last 400 frames (which span the final 4 ns of whole simulation) were used. Amber module ptraj was used to accomplish these analyses. The visualizations of the final dendrimer structure were performed using UCSF Chimera software.[10]

Structural characteristics of mPPIg5 dendrimer obtained from molecular modelling

mPPIg5 activity is governed by the spatial distribution of functional groups and units under specific conditions (e.g. solvent, temperature, pressure, pH) in addition to being governed by the primary structure of mPPIg5. In order to obtain detailed information about the 3D structure of this macromolecule in water we performed 34 ns long molecular dynamics simulation (NPT) of the water solvated mPPIg5 model. Then we calculated size characteristics of this macromolecule (Rg, Rmax) and spatial distribution of different parts of studied system with respect to the dendrimer center. The mPPIg5 dendrimer took a spherical shape and estimated values of the average Radius of gyration (Rg) and the Maximal dendrimer atom distance from dendrimer center (Rmax) are 21.1 Å and 33.3 Å (Figure S15).

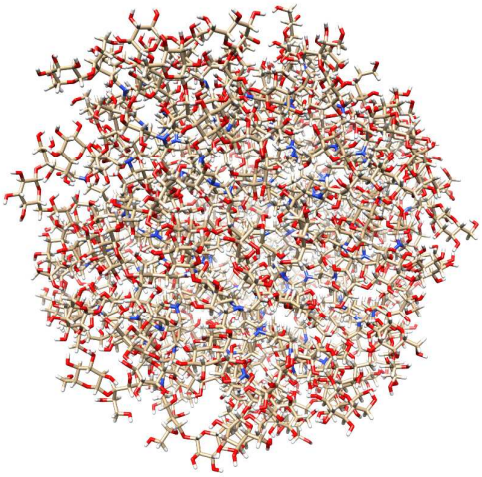

Figure S15. Overall structure of simulated mPPIg5 dendrimer presented as stick model (oxygens - red , nitrogens – blue, carbons – beige, hydrogens - white).

The radial distribution functions of different structural parts of the simulated system (including water) with respect to 2 central carbons from the dendrimer core were calculated to determine their radial densities (Figure S16).

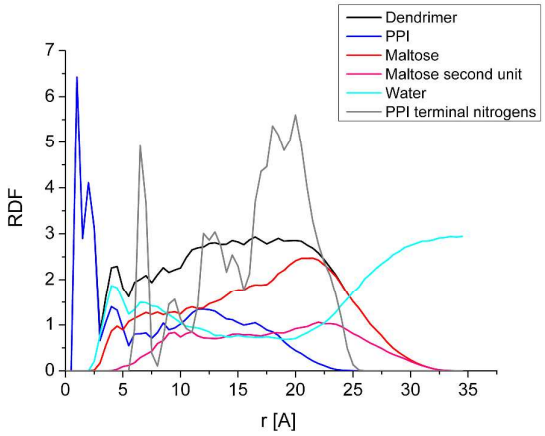

Figure S16. Radial distribution function of all dendrimer atoms (in black): PPI scaffold (in blue), maltose atoms (in red), terminal glucose units of the maltose units atoms (in pink), water (in cyan), and PPI terminal (originally the primary) PPIg5 nitrogens (in grey, here the density is multiplied by 100) with respect to two central carbon atoms from the dendrimer core.

When RDF profiles are averaged over a time interval, they also reflect the structure stability. This means that stable structure elements appear in all time samples at the same place/distance from the central atoms which supports a higher value of RDF averaged over these time samples. The maximal distance of dendrimer atoms from it's center is about 33 Å

(in agreement with Rmax direct calculation average reported above), while the PPI portion has maximal radius of about 25 Å. The water molecules can penetrate very close to the dendrimer core where they partially occupy the central cavities. The radial distribution function of specifically chosen peripheral groups or part structures of peripheral groups may also be used to examine backfolding. For this purpose we calculated separate density profiles for all maltose atoms. Alternatively, the atoms constituting the second (final) glucose ring in the attached maltose unit were calculated, while the first open glucose unit in the maltose is in an open state and bound to the PPI scaffold. The corresponding profiles (those in red and pink color in Figure S16) demonstrate that the maltose residues are distributed not only on the dendrimer surface, but also within the dendrimer structure. This is largely a consequence of backfolding of the parental PPIg5 during it's modification with maltose. This phenomenon is illustrated by the distribution of peripheral PPI nitrogens (see grey profile in Figure S16) which are connected to maltose units, although the same distribution for the original parental PPIg5 may be slightly different. Orientation of individual PPI peripheral residues also plays an important role. It should be noted that the maltose molecules nearest to the dendrimer core presented in the model, may not be present in the case of real mPPIg5 molecules. This is due to the fact that PPI peripheral units on backfolded branches in all probability remain unfunctionalized during the process of maltose modification of PPIg5 under experimental conditions. These "imprisoned" and positionally stable peripheral units mainly correspond to the first sharp grey peak in Figure S16 (located mainly in the center). To help determine the number of maltose residues located in the interior of the dendrimer structure, we identified and visualized the second glucose rings of the maltose residues (Figure S17), considering them as terminal groups in the attached maltose.

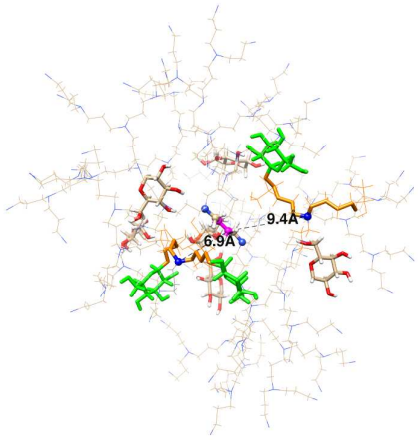

Figure S17. Visual representation of the terminal glucose rings (stick) of maltose which have at least one atom less than 10 Å from the central carbon (coloured in magenta) of PPI. Glucose rings coloured in green belong to maltose molecules which have at least one atom of their starting part (belonging to the open glucose ring (orange) attached to PPI scaffold) closer than 5 Å from the central carbon atom. PPI structure is represented by a wire background. Dendrimer core is in ball & stick representation. Both central carbons used for RDF are in magenta.

As we can see from Figure S17, there are 9 maltose molecules having at least one atom from the terminal glucose ring closer than 10 Å from the dendrimer central carbon atom. Moreover 3 of these maltoses have their starting part "buried" partially in 5 Å neighbourhood of the dendrimer center (those in green). In reality, it is unclear whether all of these "inner" maltose molecules are present in mPPIg5. As previously mentioned, backfolded PPI peripheral groups (connected with "green maltoses" in the theoretical calculation experiment (Fig S17)) may in reality stay unmodified. In Scheme 1A in the main manuscript we examined whether some of the "inner" maltose units may contribute to the surface composition of the dendrimer and show that their effect is minor.

Scheme 1A also illustrates how the molecular surface is highly dissected. This means the presence of "hills", "valleys" and even "tunnels". Evidently, "inner" sugar residues can make a minor contribution to the surface composition, though their contribution to surface activity is rather limited and strongly dependent on the experimentally given application (e.g. in the case of interaction with some ligands: the ligand size, shape and flexibility will determine this contribution).

16 References

(1) Morgner, N.; Barth, H.; Brutschy, B. A New Way To Detect Noncovalently Bonded Complexes of Biomolecules from Liquid Micro-Droplets by Laser Mass Spectrometry. *Aust. J. Chem* **2006**, *59 (2)*, 109-114.

(2) Klajnert, B.; Appelhans, D.; Komber, H.; Morgner, N.; Schwarz, S.; Richter, S.; Brutschy, B.; Ionov, M.; Tonkikh, A. K.; Bryszewska, M. The influence of densely organized maltose shells on the biological properties of poly (propylene imine) dendrimers: new effects dependent on hydrogen bonding. *Chemistry–A European Journal* **2008,** *14 (23)*, 7030-7041.

(3) Case, D. A.; Darden, T. A.; Cheatham, T. E. III Simmerling, C. L.; Wang, J.; Duke, R. E.; Luo, R.; Walker, R. C.; Zhang, W.; Merz, K. M.; Roberts, B.; Hayik, S.; Roitberg, A.; Seabra, G.; Swails, J.; Goetz, A. W.; Kolossvai, I.; Wong, K. F.; Paesani, F.; Vanicek, J.; Wolf, R. M.; Liu, J.; Wu, X.; Brozell, S.R.; Steinbrecher, T.; Gohlke, H.; Cai, Q.; Ye, X.; Wang, J.; Hsieh, M.-J.; Cui, G.; Roe, D.R.; Mathews, D.H.; Seetin, M.G.; Salomon-Ferrer, R.; Sagui, C.; Babin, V.; Luchko, T.; Gusarov, S.; Kovalenko, A. Kollman, P. A. (2012), *AMBER 12*, University of California, San Francisco.

(4) Jakalian, A.; Bush, B. L.; Jack, D. B.; Bayly, C. I. *J. Comput. Chem.* **2000**, *21*, 132-146.

(5) Wang, J.; Wolf, R. M.; Caldwell, J. W.; Kollman, P. A.; Case, D. A. *J. Comput. Chem.* **2004**, *25*, 1157-74.

(6) Kirschner, K. N.; Yongye, A. B.; Tschampel, S. M.; Daniels, C. R.; Foley, B. L.; Woods, R. J. *J. Comput. Chem.* **2008**, *29*, 622-655.

(7) Ryckaert, J. P.; Ciccotti, G.; Berendsen, H. J. C. *J. Comput. Phys.* **1977,** *23*, 327-341.

(8) Wu, X.; Brooks, B. R. *Chem. Phys. Lett.* **2003,** *381*, 512-518.

(9) Darden, T.; Perera, L.; Li, L.; Pedersen, L. *Structure* **1999**, *7*, R55–R60.

(10) Pettersen, E. F.; Goddard, T. D.; Huang, C. C.; Couch, G. S.; Greenblatt, D. M.; Meng, E. C.; Ferrin, T. E. *J. Comput. Chem.* **2004**, *25*, 1605-1612.